

XN-NF-621 (NP) (A)
REVISION 1

EXXON NUCLEAR DNB CORRELATION FOR PWR FUEL DESIGNS

OCTOBER 1983

RICHLAND, WA 99352

EXXON NUCLEAR COMPANY, Inc.

8311170200 831104
PDR ADOCK 05000316
P PDR

XN-NF-621(NP)(A)
Revision 1
Issue Date: 10/21/83

EXXON NUCLEAR DNB CORRELATION
FOR PWR FUEL DESIGNS

This is the approved version of Document XN-NF-621(NP)(A), Revision 1, and has been prepared in accordance with NRC guidance.

EXXON NUCLEAR COMPANY, Inc.



UNITED STATES
NUCLEAR REGULATORY COMMISSION
WASHINGTON, D. C. 20555

APR 12 1983

Dr. Richard B. Stout, Manager
Exxon Nuclear Company
2101 Horn Rapids Road
P. O. Box 130
Richland, Washington 99352

Dear Dr. Stout:

Subject: Acceptance for Referencing of Licensing Topical Report
XN-NF-621(P), Revision 1, "Exxon Nuclear DNB Correlation
for PWR Fuel Designs"

We have completed our review of the subject topical report submitted May 5, 1982 by Exxon Nuclear Company (ENC) letter GFO:034:82. We find this report is acceptable for referencing in license applications for LWR Plants to the extent specified and under the limitations delineated in the report and the associated (NRC) evaluation which is enclosed. The evaluation defines the basis for acceptance of the report.

We do not intend to repeat our review of the matters described in the report and found acceptable when the report appears as a reference in license applications except to assure that the material presented is applicable to the specific plant involved. Our acceptance applies only to the matters described in the report.

In accordance with established procedures (NUREG-0390), it is requested that ENC publish accepted versions of this report, proprietary and non-proprietary, within three months of receipt of this letter. The accepted versions should incorporate this letter and the enclosed evaluation between the title page and the abstract. The accepted versions shall include an -A (designating accepted) following the report identification symbol.

Dr. Richard B. Stout

-2-

APR 12 1983

Should our criteria or regulations change such that our conclusions as to the acceptability of the report are invalidated, ENC and/or the applicants referencing the topical report will be expected to revise and resubmit their respective documentation, or submit justification for the continued effective applicability of the topical report without revision of their respective documentation.

Sincerely,

Cecil O. Thomas

Cecil O. Thomas, Chief
Standardization & Special
Projects Branch
Division of Licensing

Enclosure:
As stated

1 INTRODUCTION

In XN-NF-621, Revision 1, Exxon Nuclear Company (ENC) presented the XNB critical heat flux (CHF) correlation which will be used to assess the thermal margin of pressurized water reactors (PWRs). The XNB is an empirical relationship which specifies CHF (i.e., the heat flux at which departure from nucleate boiling, DNB, occurs) as a function of local coolant conditions and fuel assembly geometry. It is based on 14 test series with a total of 714 data points and three different PWR fuel vendor designs. The 14 test series include variations in grid design, heated length, grid span, rod diameter, and axial and radial power distributions.

The local coolant conditions in the rod bundle were calculated using the XCOBRA-IIIC computer code which is described in XN-NF-75-21(P) and the range of coolant conditions tested were typical of an operating PWR.

Based on the XNB's ability to predict the test data, Exxon has proposed a departure from nucleate boiling ratio (DNBR) limit of 1.17 for the correlation. This limit corresponds to a 95% probability of not experiencing DNB at a 95% confidence level. The comparable value for the W-3 correlation, which is presently used by ENC, is 1.30.

2 DESCRIPTION OF CORRELATION

The basic form of the XNB correlation is as follows:

$$q''_{\text{uncorrected}} = A + B * \text{HLOC} \quad \text{eq. (1)}$$

where $A = f(\text{pressure, mass velocity, inlet subcooling})$

$B = f(\text{pressure, mass velocity, local enthalpy})$

HLOC = Reduced local enthalpy

= Local Enthalpy/906.00

All of the parameters used in the XNB are reduced using the critical properties of water (i.e., the water properties at the critical pressure, 3208.2 psi) and using the above method for HLOC.

Additional factors are used as part of the correlation to account for non-uniform axial power distributions, geometry differences such as spacer pitch and mixing vane loss coefficients, and differences in heated lengths. The final form of the XNB is:

$$q''_{\text{critical}} = (q''_{\text{uncorrected}})^* \text{Correction Factors} \quad \text{eq. (2)}$$

The procedure for using the XNB is to initially calculate the heat flux using equation (1), determine the appropriate correction factors, calculate CHF using equation (2), and determine the DNBR, which is the ratio of the actual heat flux to predicted CHF.

The ranges over which Exxon is requesting the XNB be applied (Chandler; January 6, 1983) are:

Pressure (psia)	1395 - 2425
Local Mass Velocity (Mlbm/hr-ft ²)	0.92 - 3.04
Local Enthalpy (Btu/lb)	594.85 - 821.24
Local Quality	-0.2 - +0.3
Heated Length (inches)	66 - 168
Grid Spacing (inches)	14.3 - 22.0
Inlet Subcooling (Btu/lb)	37.2 - 336.34

It will also be used for the following geometries:

Vendors:	Exxon Nuclear Combustion Engineering Westinghouse
Fuel Design:	Non-Mixing Vane Mixing Vane
Equivalent Hydraulic Diameter (inches)	0.177 - 0.612
Equivalent Heated Diameter (inches)	0.463 - 0.528

The test series and their associated fuel rod arrays are:

Vendor	Rod Array	Test Series
Westinghouse/ Exxon	14x14, 15x15	ENC-3, 4, and 5 ROSAL-2, 4, 7, and 8
Exxon	17x17	ENC-6
Combustion Engineering	16x16	CE-47, CE-59
Westinghouse	17x17	WH-162 and 164

3 STAFF EVALUATION

3.1 Scope of Review

The staff review of XN-NF-621, Revision 1 included an independent audit of the subchannel calculations performed to determine the local coolant conditions in the rod bundle for all 714 data points. This was performed using the COBRA-IV computer code which was derived from and is an ancillary of the COBRA-IIIC program. Our review also included a statistical analysis of the calculated results and a review of the methodology used in combining the XCOBRA-IIIC code and the correlation. During the review, requests were made for data clarification and additional or corrected information was received in several areas.

The above reviews were performed by the Idaho National Engineering Laboratory (INEL) under the direction of a cognizant staff member.

3.2 Results of Audit Calculations

The results of the INEL audit calculations are presented in Tables 1 and 2. Table 1 is a comparison of the local conditions at which CHF was predicted as determined by the XCOBRA-IIIC and COBRA-IV codes for a limited number of data points. The comparison indicates good agreement between the two codes and either could be used to establish the local conditions required for the development of a CHF correlation.

Table 2 is a comparison of the mean and standard deviation for each of the data sets and the total population. This comparison shows good agreement for the overall values but contains discrepancies in many of the individual data sets. The possible ramifications associated with these differences are described in the statistical analysis discussion contained in this report.

During our review, the staff requested that Exxon provide a description of how the local conditions for the XNB were determined including a discussion of the subchannel code used, subchannel modeling, axial nodalization, and input assumptions. Exxon responded that the XCOBRA-IIIC code was used to calculate the local coolant conditions. XCOBRA-IIIC is a derivative of the COBRA-IIIC code which was developed at Battelle Pacific Northwest Laboratory. The modifications made by Exxon to COBRA-IIIC include minor improvements in the solution technique, the addition of calculational options, and operational modifications such as streamlining code input.

Exxon further stated that the friction factors used were determined from pressure drop measurements performed on ENC test sections or estimated for geometries for which ENC does not have detailed test data. These loss coefficient estimates are based on the experience gained from measuring actual fuel bundles of Westinghouse or Combustion Engineering (C-E) designs. They also reported that sensitivity studies of CHF test data showed negligible influence on predicted conditions when the form loss coefficients were varied by as much as 15%.

The mixing values ($\frac{B_s}{D}$) chosen were based on spacer design and are dependent on a particular fuel type. These values were determined experimentally for the ENC designed fuel while for non-Exxon fuel a lower bounding value was used for mixing vane grids. For example, in analyzing, the Westinghouse "L" grid design a lower value of 0.010, which was obtained from WCAP-8030-A, was used.

Based on our review of the above information, the staff concludes that the approach taken by Exxon in determining the local conditions used in developing the XNB correlation are acceptable. The XCOBRA-IIIC code is still under staff review, and any limitations resulting from this review will be addressed in our safety evaluation report on XN-NF-75-21(P), Revision 2.

The INEL audit calculations were performed using the same friction factor correlation, two-phase flow correlation, crossflow resistance, momentum turbulent mixing factor, pitch to length parameter, inlet enthalpy and inlet mass velocity as Exxon.

Our review also included an analysis of the correction factors used in the XNB development and the determination of these factors in actual reactor application. Based on this review, we have concluded that the method used to calculate these parameters and their values used in determining the DNBR limit are acceptable.

However, it is the opinion of the staff and our consultant that a change in these parameters, such as determining their values using a prototype and then a full scale bundle, may increase the uncertainty in both the code's prediction of local coolant conditions and the correlations prediction of CHF. This may significantly alter the statistical analyses on which the DNBR limit is based. Therefore, we conclude that the values of these parameters used in the development of the XNB must be used in licensing analyses.

For the uniform heat flux tests, ENC used the end of the heated length as the CHF location while the experiments showed that for the same tests, CHF occurred upstream of the end of the heated length. When asked to justify using this technique in determining the DNBR Exxon responded that the worst local conditions calculated for a bundle having a uniform axial power distribution (APD) are at the end of the heated length. In order to maintain a consistent path between test analysis and reactor design and based on the fact that the DNBR location in a reactor is determined by the code and is not known a priori, the procedures used to determine the DNBR for those tests where burnout occurred upstream of the heated length is acceptable. We have reviewed the additional information provided by ENC and have concluded that the method used by Exxon in determining DNBR is acceptable since the DNBR limit is dependent on the ability of the subchannel code to predict local conditions which produce CHF.

An additional area of concern raised by the staff on the uniform heat flux tests was why CHF occurred at the thermocouple upstream of the end of the heated length rather than at the end of the heated length where the highest quality region should occur. Exxon stated that burnout is a function of the

location of the spacer grid and that the grids will improve heat transfer for a distance of 20 or more rod diameters downstream of the spacer. Because the spacer was located slightly downstream of the end of the heated length, heat transfer above the spacer would improve while the local hydraulic conditions downstream of the grid would be more severe. Therefore, for the experimental data in question, the effects of the spacer grid dominated the occurrence of CHF even though a higher quality may occur at the end of the test bundle. The staff has reviewed this information and concludes that ENC has acceptably addressed our concerns on this issue.

Finally in the area of test procedures, the staff requested that Exxon provide a discussion on how the rate of power was increased, what post-test inspections were performed, and what, if any, duplicate runs were made to establish continued integrity of the test bundle. In response to this concern, ENC stated that the power was manually raised in the CHF tests by an increment of less than 1% and held constant until conditions became stable. This process was repeated until CHF occurred. They further stated that duplicate runs were made to establish continued integrity. As an example, they cited the ENC-6 tests, where replicate points were taken during the test and one in between point was taken at the end of the test to confirm continuity and consistency of the test data from beginning to end. At the end of the tests, post-test inspections were performed and, for example, on the ENC-6 bundle there were no visible signs of hot spots on the rods. Based on our review of this information, the staff has concluded that the CHF tests were performed in an acceptable manner.

Our review of the statistical characterization of the XNB results dealt mainly with the method used by Exxon to statistically analyze the data and a review of the analyses. The statistical method used by ENC was to evaluate the predicted-to-measured (P/M) ratio of CHF data. Since in previously approved correlations, the measured-to-predicted (M/P) ratio was used to determine the 95/95 limit, Exxon was asked to justify their technique. ENC responded that the procedure used in determining the 95/95 limit assumed a normal distribution. Transforming the data from P/M to M/P yields two distributions for comparison, both of which may be normal or both may depart from normality. As a verification on the 95/95 limit for the P/M data, Exxon

performed a distribution free estimate of the limit and determined the value to be 1.177. For the reverse ratio, and using their original statistical approach, Exxon calculated that 95/95 limit for the M/P data, when a normal distribution is assumed, is 1.191.

ENC further stated that the non-parametric estimate of the 95/95 limit, 1.177, does not make complete use of the actual distribution, and therefore this limit will bound the 95/95 limit obtained from the actual distribution. By considering the first four moments of the P/M data ENC found that the actual distribution is a gamma distribution. On the other hand, the use of the M/P data is overly conservative since, the actual value of the 95/95 limit for the P/M data, when the appropriate distribution is used, lies at some value below the non-parametric limit of 1.177. ENC also stated that the DNBR reported for licensing analyses is defined as P/M ratio. Based on our review of the above information, the staff has concluded that the analysis of the P/M data is acceptable.

As part of the review, the staff requested that Exxon demonstrate that each of the samples, e.g., test series, belong to a single population. ENC responded by initially performing a Bartlett test for homogeneity of variance (Chandler; August 26, 1982). The breakdown was based on both vendor design and fuel assembly geometries. The results of this test showed that the variances do differ among geometry types.

Exxon also performed a K-sample Squared Ranks test of variance using the above groupings (Chandler; August 26, 1982). Results for the population of 6 samples and 5 degrees of freedom indicated that at least two of the variances were unequal. By removing the ROSAL, ENC-1, and 2 data, Exxon found that there exists a significance level between 2.5% and 5.0% that the remaining data were from the same population. Finally, ENC removed the ENC-3, 4, and 5 data and analyzed the remaining population. Based on the results of the third analysis, Exxon concluded that the data comprised of 3 samples and 2 degrees of freedom were likely identical.

An analysis of the means and a comparison of variance analysis showed that for an equivalent sample size of 83.7 with 378.7 degrees of freedom the mean is 0.98502 with a standard deviation of 0.09847. Based on this mean and standard deviation the 95/95 DNBR limit would be 1.168.

The final analysis performed by ENC was the determination of a DNBR limit excluding that data which had the greatest possibility of being from a different population. For all sections less the ROSAL and ENC 1 thru 5 data the DNBR limit was 1.169 while for all sections less the ENC-6, WH-162, WH-164, CE-47, and 49 data, the DNBR limit was 1.176.

The results of the above tests lead ENC to conclude that the data could be treated as a single population and that the 1.17 DNBR limit would cover any deviation within the data sets.

In order to ascertain the validity of these conclusions, INEL performed a series of F-tests to identify any systematic variation among the test series. The tests were performed at a 99% confidence level. Based on the F-test, INEL concluded that there was a variance among tests of different geometries. Additionally, INEL performed a one-way analysis of variance using the ungrouped test series.

For the one-way analysis, INEL used the groupings reported by ENC and calculated a F-ratio of 24.03 for six samples with five and 708 degrees of freedom for the numerator and denominator. This result shows that there is a variance among the tests when they are grouped by geometry type. Removing data sets WH-162, WH-164, ENC-3, 4, and 5 resulted in an F-ratio of 2.40 with three and 392 degrees of freedom for the numerator and denominator. This indicates that the remaining data have a probability of between 5% and 10% of being in the same population.

A second one-way analysis of variance was performed on the ungrouped data. The results of this test are presented in Table 3 and indicate that ENC-1, ENC-2, ENC-6, ROSAL-2, ROSAL-7, ROSAL-8, WH-162, CE-47 and CE-49 are probably of the same population while test series ENC-3, ENC-4, ROSAL-4, and WH-164 are

of a second population. ENC-5 is a unique test series and does not fall into either population. Using the above populations, a DNBR limit of 1.21 for the ENC-1, ENC-2, etc. population was determined while the ENC-3, ENC-4, etc. population has a 95/95 limit of 1.133.

Figure 1 is a histogram of the total data set and it shows that the overall population is approximately normally distributed. Histograms for the individual samples (EGG-NTAP-6167) show that ENC-3, ENC-4, ENC-5, ROSAL-4 and WH-164 are skewed to the left of the population mean.

Further analyses were performed to determine if there was a reason for the groupings obtained from the one-way analysis of variance. A number of groupings were examined using different bases such as rod diameter, grid spacing, radial power distribution, axial power distribution, KLOSS, and an unheated guide tube in the bundle. These studies showed no uniqueness in either grouping.

A second evaluation revealed that the modeling of the guide tube was an influence in determining the above grouping. For those bundles containing an unheated guide tube, CHF experimentally occurred in a channel that contained the guide tube; however, in predicting CHF, Exxon often reported burnout in a channel other than the one with the guide tube. Since the guide tube is an unheated wall, CHF occurs at less severe local conditions and has a lower value. If CHF is predicted in a typical channel, four heated rods, when it actually occurred in a guide tube channel, this would be nonconservative. The reason for this is that the predicted local conditions are greater than the conditions which experimentally produced CHF; therefore, the analytical results show that you can go to a higher power than you actually achieved.

Table 4 presents a summary of the test series that have one or more unheated guide tubes. For all of the series reported in Table 4 ENC predicted CHF in the COBRA hot channel rather than the experimental channels listed in the table. This indicates that the reason ENC-3, ENC-4, and ENC-5 do not belong to the population may be the difference in the channel for the predicted and measured CHF. Test series ENC-6 does not fall from the population because the

difference between the COBRA-IV experimental hot channel and the guide tube channel is only 3.0% and the sample mean is closer to the expected mean of 1.0.

In addition to the above analyses, the INEL audit calculations revealed that the ENC-1, 2, 3, 4, 6, CE-59, and ROSAL-8 test series were biased with inlet pressure. For pressures less than 1800 psia the correlation predictions tend to be scattered about some value less than 1.0 while for data above 1800 psia the data is randomly scattered about 1.0. This indicated that the correlation under predicts CHF for the lower pressures but is reasonably accurate for pressures above 1800 psia. Based on this review, the staff has concluded that although these test series statistically belong to one of the two populations, excluding the ENC-5 population, the fact that they are biased with pressure may preclude them from being placed in either population.

Also, the staff statistically analyzed the six different geometry types reported by Exxon. Table 5 contains the results of our analysis based on a geometric characterization. These results show that for the ENC-1 and -2 population the mean, standard deviation, and 95/95 limit are much greater than the mean, standard deviation, and 95/95 limit of the remaining populations when they are compared to the same parameters of the total population.

Based on our review of the ENC statistical analyses, our consultant's analyses, and the result of the staff's statistical analyses, we requested additional information from Exxon which justified treating the 14 samples as one population.

In response to our concerns, Exxon provided plots of DNBR versus inlet pressure for those test series that the staff felt were biased with pressure (Chandler; December 16, 1982). Based on their own pressure plots ENC concluded that there was no significant systematic trends with pressure. We have reviewed the information submitted in the December 16, 1982 letter and have concluded that there is a small trend with pressure; however, the trend is random in nature and does not exhibit any systematic characteristics. Therefore, the staff concludes that the ENC-1, 2, 3, 4, 6, CE-59, and ROSAL-8 test series

need not be treated as a single population due to the trends in pressure, since these trends are not systematic.

With respect to the statistical analyses, Exxon requested that the data be reviewed as two separate populations (Chandler; December 22, 1982). One of the populations would be comprised of the test series representing 16x16 and 17x17 arrays (CE-47, CE-59, WH-164, WH-162, and ENC-6) while the second population would represent the 15x15 bundles. As justification for requesting this breakup, ENC provided the range of test conditions and axial power distributions found in each population.

A review of the 16x16 and 17x17 data base showed that only a chopped cosine and uniform axial power distribution (APD) were present. It is the position of the staff that all possible power distributions expected throughout an operating cycle be used in the development of any CHF correlation. Since the 16x16 and 17x17 do not include either an upskew or downskew APD, Exxon cannot remove those test series, e.g. the 15x15 array, that have the upskew APDs. Therefore, the 15x15 test series must remain in the data base until ENC provides additional data for the 16x16 and 17x17 test series which contain an upskew and/or downskew APD.

In a modified response (Chandler; January 3, 1983) Exxon requested that test series ENC-1 and ENC-2 be removed from the data base. The reason for eliminating this data was that ENC-1 contained minimum grids that were not representative of any grid being manufactured by ENC, Westinghouse or CE while ENC-2 had a uniform axial and radial power distribution that was atypical of actual reactor conditions. ENC further stated that a statistical analysis of the data was performed using the populations reported by INEL. The results of these evaluations showed that the worst 95/95 limit was 1.17 for the population containing the CE-47, -59, WH-162, ENC-2, ROSAL-2, -7, and -8 test series. Based on these results, we have concluded that the proposed grouping of data which results in a DNBR limit value of 1.17 is acceptable.

4 CONCLUSION

The staff has reviewed XN-NF-621, Revision 1 and the additional supporting information submitted by Exxon Nuclear Company. Based on this review, we have concluded that XNB correlation is acceptable for use in reactor licensing applications. We have also concluded that the 95/95 DNBR limit of 1.17 reported by Exxon is acceptable. These conclusions are based on the following:

- (1) The subchannel code used, XCOBRA-IIIC, is acceptable for predicting local coolant conditions used in the development of a CHF correlation. This is based on a comparison of XCOBRA-IIIC with the staff's audit code COBRA-IV. Since the XCOBRA-IIIC is still under staff review, any limitations resulting from its use will be addressed in our safety evaluation report on the code.
- (2) An independent audit, performed by our consultant INEL, using a different subchannel code yielded similar results.
- (3) The DNBR data has been statistically characterized in an acceptable manner.
- (4) The 95/95 limit is based on three separate populations that were recommended by our consultant; therefore, the 95/95 limit of one population will be conservative when compared to the limit of a population containing all of the test data.

We will require that the correction factors used in analyzing the CHF test data and the mixing factors used in the data reduction be used in reactor design applications, since a change in these factors may alter the code and correlation uncertainties associated with the prediction of CHF. This in turn may raise or lower the 95/95 DNBR limit. Therefore, if any of these parameters are changed, ENC must provide a description of the change and

sufficient justification which warrants making this change. Additionally, Exxon should provide the test data which justifies using the XNB on fuel designs not contained in the data base or acceptable justification on why the XNB is applicable to this fuel type. For example, Exxon manufactured fuel for CE reactors is not present in the data base. ENC must provide additional test data for these fuel bundles or a quantified justification of the XNB's applicability to this bundle type.

Finally, it should be noted that the DNBR limit does not include any adjustment which is required when a mixed core, e.g. a core with geometrically different fuel types, is analyzed.

5 REGULATORY POSITION

The staff concludes that the XNB CHF correlation as described in XN-NF-621, Revision 1 is acceptable for use in licensing application when it is used with the XCOBRA-IIIC code and within the range of application reported in Section 2.2 of this safety evaluation report. We also conclude that the S5/95 limit of 1.17 associated with the XNB is acceptable. Use of the correlation should be within the limitations described in the previous section.

Based on our review, the staff finds XN-NF-621, Revision 1 an acceptable and referential report with the restrictions noted in the above paragraph.

Table 1: Comparison of Local Conditions

Case	Enthalpy		Quality		Void Fraction		Mass Flux	
	XCOBRA-III	COBRA-IV	XCOBRA-III	COBRA-IV	XCOBRA-IIIIC	COBRA-IV	XCOBRA-IIIIC	COBRA-IV
ENC-3-63	656.57	656.49	0.077	0.077	0.610	0.594	1.9046	1.9434
ENC-4-28	703.28	705.78	0.167	0.167	0.709	0.712	1.4897	1.5210
ENC-6-42	616.44	628.00	0.00	0.007	0.318	0.350	2.8655	2.8998
ROSAL-2-18	612.57	627.50	0.001	0.027	0.550	0.554	1.8674	1.8809
ROSAL-2-9	622.44	636.52	0.018	0.043	0.561	0.566	1.9409	1.9601

Table 2: Comparison of Mean and Standard Deviation

Test Section	Number of Data Points	Mean (Meas./Pred)		Standard Deviation	
		XCOBRA-IIIC	COBRA-IV	XCOBRA-III	COBRA-IV
CE-47	96	1.028	1.0300	0.0741	0.0804
CE-59	89	1.023	1.0500	0.0820	0.1020
WH-164	53	0.950	0.9727	0.0677	0.0682
WH-162	53	0.992	1.0032	0.0845	0.0736
ROSAL-2	28	0.976	0.9995	0.118	0.0990
ROSAL-4	26	0.933	0.9689	0.0843	0.0832
ROSAL-7	11	0.970	1.0383	0.1043	0.1210
ROSAL-8	32	1.001	1.0586	0.0987	0.1070
ENC-1	28	1.040	1.0504	0.1212	0.1220
ENC-2	24	0.993	1.0119	0.1093	0.1090
ENC-3	73	0.994	0.9458	0.1029	0.0923
ENC-4	80	0.985	0.9712	0.1196	0.112
ENC-5	59	0.911	0.8956	0.0848	0.0811
ENC-6	<u>62</u>	<u>0.995</u>	<u>1.0071</u>	<u>0.0749</u>	<u>0.0868</u>
Total Population	714	0.985	0.99614	0.09847	0.1030

Table 3: One Way Analysis of Variance

Test Series Grouping	F-Ratio	Probability of Being in Same Population
ENC-1, -2, -6		
ROSAL-2, -7, -8		
WH-162, CE-47, -59	2.47	1 - 2.5%
ENC-1, -2, -4, -6		
ROSAL -2, -4, -7, -8		
WH-162, -164		
CE-47, CE-59	5.57	---
ENC-1, -2, -3, -4, -6		
ROSAL-2, -4, -7, -8		
WH-162, -164		
CE-47, -59	7.84	---
ENC-3, -4, -5		
ROSAL-4, WH-164	7.39	---
ENC-3, -4		
ROSAL-4, WH-164	1.23	>10%

Table 4: Comparison of Test Series With Unheated Guide Tubes

Test Series	Number of Experimental CHF Predictions		Explanation
	COBRA-IV Hot Channel ¹	COBRA-IV Channel Other Than Hot Channel	
WH-162	All	-0-	As expected.
ENC-6	20	42	The 42 channels are 3% cooler than the hot channel.
ENC-3	18	53	Five of the indications occur in a channel with 5% less power, 21 in a channel with 0.4% less power and the remaining in a channel with 23% less power.
ENC-4	30	50	Seven of the 50 indications were in a channel with 0.20% less power while the remaining 43 were in a channel with 22% less power.
ENC-5	4	53	Twenty-five of the 53 indications occur in a channel with 0.9% less power while the remaining 28 are in a channel with 22% less power.
CE-47	82	14	The 14 indications occur in a channel with 0.3% less power.
CE-59	85	4	The 4 indications occur in a channel with 0.1% less power.

¹ENC predicts all CHF's in this channel.

Table 5: Comparison of 95/95 Limit Based on Geometry

Geometry Grouping	Mean	Standard Deviation	95/95 Limit
CE-47, CE-59	1.0256	0.0778	1.169
WH-162, WH-164	0.9710	0.0791	1.123
ENC-6	0.995	0.0749	1.146
ROSAL-2, 4, 7, 8	0.9720	0.1021	1.169
ENC-1, ENC-2	1.0183	0.1173	1.259
ENC-3, ENC-4, ENC-5	0.9503	0.0865	1.109
Total Population	0.985	0.0985	1.163

6 REFERENCES

6.1 Topical Reports

XN-NF-621, Revision 1 "Exxon Nuclear DNB Correlation for PWR Fuel Designs," Exxon Nuclear Company, April 1982.

XN-NF-75-21(P), Revision 2, "XCOBRA-IIIC: A Computer Code to Determine the Distribution of Coolant During Steady-State and Transient Core Operation," Exxon Nuclear Company, September 1982.

WCAP-8030-A, "Application of Modified Spacer Factor to L Grid Typical and Cold Cell DNB," Westinghouse Electric Corporation, January 1975.

6.2 Other References

Ambrosek, R. G., C-C Tsai, and R. D. Wadkins, "Exxon Nuclear DNB Correlation Review," EGG-NTAP-6167, EG&G Idaho, INC., February 1983.

J.C. Chandler (ENC) to H. Bernard (NRC), Subject: "XN-NF-621(P), 'Exxon Nuclear DNB Correlation for PWR Fuel Designs,' Revision 1," August 26, 1982.

J.C. Chandler (ENC) to J.J. Holonich (NRC), Subject: "XN-NF-621, Revision 1, 'Exxon Nuclear Company DNB Correlation for PWR Fuel Designs,' April 1982," December 9, 1982.

J.C. Chandler (ENC) to L.E. Phillips (NRC), Subject: "XN-NF-621, Revision 1, 'Exxon Nuclear Company DNB Correlation for PWR Fuel Designs,' April 1982," December 16, 1982.

J.C. Chandler (ENC) to L.E. Phillips (NRC), Subject: "XN-NF-621, Revision 1, 'Exxon Nuclear Company DNB Correlation for PWR Fuel Designs,' April 1982," December 23, 1982.

J.C. Chandler (ENC) to L.E. Phillips (NRC), Subject: "XN-NF-621, Revision 1, 'Exxon Nuclear Company DNB Correlation for PWR Fuel Designs,' April 1982," January 3, 1983.

J.C. Chandler (ENC) to L.E. Phillips (NRC), Subject: "XN-NF-621(P), Revision 1, 'Exxon Nuclear DNB Correlation for PWR Fuel Designs,' April 1982," January 6, 1983.

EXXON NUCLEAR DNB CORRELATION
FOR PWR FUEL DESIGNS

Prepared by: *R. B. Macduff*
R. B. Macduff

7 April 82
Date

Approved by: *T. W. Patten*
T. W. Patten, Manager, Fuel Testing

4/12/82
Date

J. F. Patterson
J. F. Patterson, Manager
Fuel Development and Testing

4/12/82
Date

J. N. Morgan
J. N. Morgan, Manager, Fuel Licensing

4/12/82
Date

G. A. Sofer
G. A. Sofer, Manager
Fuel Engineering & Technical Services

20 APR 82
Date

G. L. Ritter
G. L. Ritter, Manager
Process and Engineering Development

4/21/82
Date

NUCLEAR REGULATORY COMMISSION DISCLAIMER

IMPORTANT NOTICE REGARDING CONTENTS AND USE OF THIS DOCUMENT

PLEASE READ CAREFULLY

This technical report was derived through research and development programs sponsored by Exxon Nuclear Company, Inc. It is being submitted by Exxon Nuclear to the USNRC as part of a technical contribution to facilitate safety analyses by licensees of the USNRC which utilize Exxon Nuclear-fabricated reload fuel or other technical services provided by Exxon Nuclear for light water power reactors and it is true and correct to the best of Exxon Nuclear's knowledge, information, and belief. The information contained herein may be used by the USNRC in its review of this report, and by licensees or applicants before the USNRC which are customers of Exxon Nuclear in their demonstration of compliance with the USNRC's regulations.

Without derogating from the foregoing, neither Exxon Nuclear nor any person acting on its behalf:

- A. Makes any warranty, express or implied, with respect to the accuracy, completeness, or usefulness of the information contained in this document, or that the use of any information, apparatus, method, or process disclosed in this document will not infringe privately owned rights; or
- B. Assumes any liabilities with respect to the use of, or for damages resulting from the use of, any information, apparatus, method, or process disclosed in this document.

EXXON NUCLEAR DNB CORRELATION
FOR PWR FUEL DESIGNS

TABLE OF CONTENTS

	<u>Page</u>
1.0 INTRODUCTION AND SUMMARY	1-1
2.0 ENC DEPARTURE FROM NUCLEATE BOILING CORRELATION	2-1
2.1 XNB CORRELATION	2-1
2.2 NON-UNIFORM AXIAL HEAT FLUX FACTOR	2-2
2.3 GEOMETRIC CORRECTORS	2-3
2.3.1 Spacer Pitch Factor	2-3
2.3.2 Mixing Vane Factor	2-3
2.3.3 Length Factor	2-4
2.4 PROCEDURE FOR USING THE XNB CORRELATION AND CORRECTION FACTORS TO PREDICT DNB HEAT FLUX	2-4
3.0 COMPARISON OF XNB AGAINST EXPERIMENTAL DNB DATA	3-1
3.1 EXXON NUCLEAR PWR DNB TEST DATA	3-1
3.1.1 Test Sections 1 & 2	3-2
3.1.2 Test Sections 3 & 4	3-2
3.1.3 Test Section 5	3-3
3.1.4 Test Section 6	3-3

3.2	C. FIGHETTI AND D. REDDY DNB DATA	3-4
3.2.1	Combustion Engineering DNB Test Data	3-4
3.2.2	Westinghouse DNB Test Data	3-5
3.3	ROSAL, ET AL TEST SECTIONS	3-5
3.4	DISCUSSION AND CONCLUSIONS OF ANALYSIS OF DNB TEST DATA ..	3-6
3.4.1	Subchannel Mixing	3-6
4.0	STATISTICAL EVALUATION	4-1
5.0	REFERENCES	5-1

APPENDICES

A	DATA SUMMARY FOR TEST SECTIONS - ENC	A-1
B	DATA SUMMARY FOR TEST SECTIONS - ROSAL	B-1
C	DATA SUMMARY FOR TEST SECTIONS - CE/WH	C-1

LIST OF TABLES

	<u>Page</u>
1.1 Summary of DNB Data Analyzed	1-3
3.1 Summary of Test Conditions	3-8
3.2 Statistical Summary	3-11

LIST OF FIGURES

1.1 Comparison of Heat Flux - ALL	1-4
3.1 Test Assembly Geometry and Local Power Distribution for ENC 1 & 2 Test Assemblies	3-12
3.2 Spacer, Pressure Tap and Thermocouple Locations for ENC 1 Test	3-13
3.3 Spacer, Pressure Tap and Thermocouple Locations For ENC 2 Test	3-14
3.4 Comparison of Heat Flux - ENC-1	3-15
3.5 Comparison of Heat Flux - ENC-2	3-16
3.6 Test Assembly Geometry and Local Power Distribution for ENC 3 & 4 Test Assemblies	3-17
3.7 Spacer, Pressure Tap and Thermocouple Locations for Tests ENC 3 & 4	3-18
3.8 Comparison of Heat Flux - ENC-3	3-19
3.9 Comparison of Heat Flux - ENC-4	3-20
3.10 Test Assembly Geometry and Local Power Distribution for ENC-5 Test Assembly	3-21
3.11 Spacer, Pressure Tap and Thermocouple Locations for ENC-5 Test Assembly	3-22
3.12 Comparison of Heat Flux - ENC-5	3-23
3.13 Test Assembly Geometry and Local Power Distribution for ENC-6 Test Assembly	3-24
3.14 Axial Power Distribution for ENC-6 Test Section	3-25
3.15 Spacer, Pressure Tap and Thermocouple Location for ENC-6 Test Assembly	3-26
3.16 Comparison of Heat Flux - ENC-6	3-27
3.17 Test Assembly Geometry and Local Power Distribution for CE-47 Test Section	3-28
3.18 Test Assembly Geometry and Local Power Distribution for CE-59 Test Section	3-29
3.19 Spacer and Thermocouple Locations for CE-59 Test Section and Spacer Locations for CE-47 Test Section	3-30
3.20 Axial Power Distribution for CE-59 Test Section	3-31
3.21 Comparison of Heat Flux - CE-47	3-32
3.22 Comparison of Heat Flux - CE-59	3-33
3.23 Test Assembly Geometry and Local Power Distribution for W-162 Test Section	3-34

LIST OF FIGURES

	<u>Page</u>
3.24 Test Assembly Geometry and Local Power Distribution for W-164 Test Section	3-35
3.25 Spacer and Thermocouple Locations for Test Sections W-162 and W-164	3-36
3.26 Axial Power Distribution for W-162 and W-164 Test Sections	3-37
3.27 Comparison of Heat Flux - WH-162	3-38
3.28 Comparison of Heat Flux - WH-164	3-39
3.29 Test Section Geometry and Local Power Distributions for ROSAL 2, 6, 7 and 8 Test Assemblies	3-40
3.30 Spacer and Thermocouple Locations for ROSAL 2, 6, 7 and 8 Test Sections	3-41
3.31 Axial Power Distributions for ROSAL Data	3-42
3.32 Comparison of Heat Flux - ROSAL-2	3-43
3.33 Comparison of Heat Flux - ROSAL-4	3-44
3.34 Comparison of Heat Flux - ROSAL-7	3-45
3.35 Comparison of Heat Flux - ROSAL-8	3-46

1.0 INTRODUCTION AND SUMMARY

Exxon Nuclear presents in this report a new correlation for assessing thermal margin in pressurized water reactors (PWRs). The thermal margin in pressurized water reactors is assessed with a correlation of the local fluid conditions which result in a sudden rise in fuel rod temperature. This temperature rise is due to a degradation of heat transfer at the rod surface which is commonly known as departure from nucleate boiling (DNB) or critical heat flux (CHF). The correlation described in this report, the XNB correlation, has been compared with data gathered at Columbia University^(2,3) with test assemblies representing several different designs, as summarized in Table 1.1.

The local fluid conditions which lead to DNB have been predicted by a subchannel analysis of the test assemblies. This analysis is performed with the XCOBRA-IIIC⁽¹⁾ computer code, which performs a simultaneous solution of equations representing the conservation of mass, momentum, and energy. The calculated local fluid conditions were used as the correlative basis in predicting the rod surface heat flux which results in DNB. The XNB correlation is comprised of a base correlation with a correcting term for non-uniform axial heat flux profile, correcting terms for fuel length, spacer pitch, and mixing vanes.

For each data point in the data base, the ratio of the heat flux predicted by the XNB correlation to that measured in the testing (DNB heat flux ratio) has been determined. A comparison of the predicted heat flux to measured heat flux for all data is shown in Figure 1.1. The average DNB ratio as well as the standard deviation have been determined to assess the accuracy of the XNB correlation. This comparison shows that a fuel rod operating with a minimum DNB ratio (MDNBR) of 1.16 is assured that with 95% confidence, there is a 95% probability of avoiding DNB.

Table 1.1 Summary of DNB Data Analyzed

Test Bundle	Grid* Type	Heated Length (feet)	Grid Span (inch)	Rod Diameter (inch)	Power Distribution		DNBR		Number Points
					Axial	Radial	Mean		
CE-47	NV	12.5	14.30	.382	UNIFORM	.97-1.14	1.028	0.0741	96
CE-59	NV	12.5	14.30	.382	COSU	.96-1.20	1.023	0.0820	89
WH-162	MV	14.	22.0	.374	COSU	.95-1.10	0.992	0.0845	53
WH-164	MV	14.	22.0	.374	COSU	.94-1.10	0.950	0.0677	53
ENC-6	MV	12.	20.5	.360	COSU	.97-1.10	0.995	0.0749	62
ENC-1	MG	6.	15.5	.413	UNIFORM	UNIFORM	1.029	.1186	28
ENC-2	NV	6.	15.5	.413	UNIFORM	UNIFORM	.983	.1084	24
ENC-3	MV	6.	15.7	.421	UNIFORM	.95-1.1	.939	.0895	73
ENC-4	MV	6.	15.7	.421	UNIFORM	.95-1.1	.985	.1196	80
ENC-5	MV	5.5	26.2	.424	UNIFORM	.95-1.08	.915	.0843	59
ROSAL-2	MV	8.	20.	.422	USINU	.95-1.15	.976	.1118	28
ROSAL-4	NV	8.	20.	.422	USINU	.95-1.15	.933	.0843	26
ROSAL-7	MV	8.	20.	.422	COSU	.98-1.05	.970	.1043	11
ROSAL-8	MV	8.	26.	.422	COSU	.98-1.03	1.001	.0987	32
							.984	0.0964	714

* Legend: NV = Non-Vaned
 MV = Mixing Vane
 MG = Minimum Grid

1-3
 XN-NF-621(NP)(A)
 Revision 1

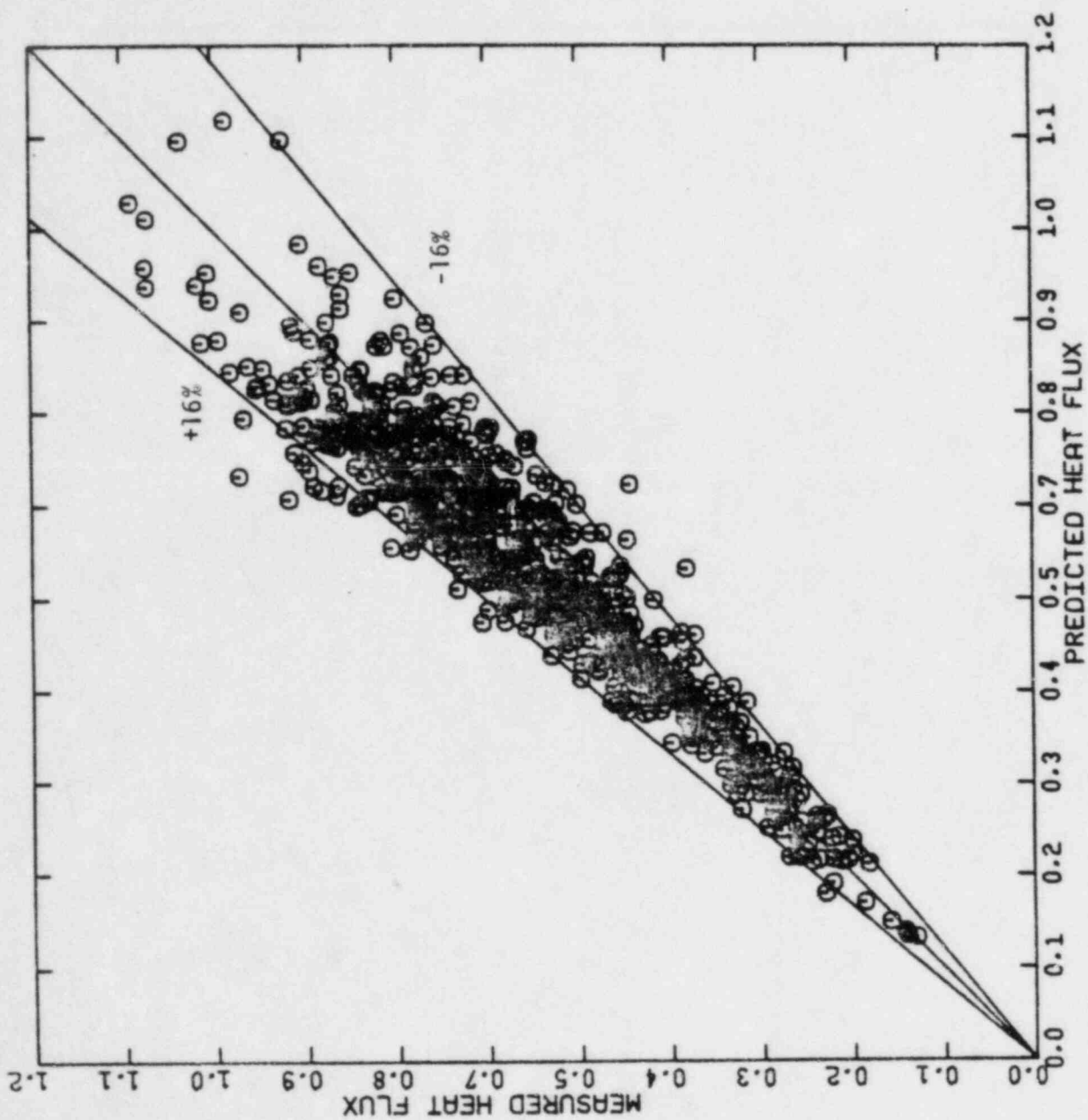


FIGURE 1.1 COMPARISON OF HEAT FLUX - ALL

2.0 END DEPARTURE FROM NUCLEATE BOILING CORRELATION

The onset of boiling transition or DNB is characterized by an abrupt decrease in the boiling heat transfer coefficient due to a change in heat transfer mechanisms. This is indicated by a temperature excursion of the heating surface. The maximum heat flux attained before boiling transition is called the critical heat flux (CHF) or departure from nucleate boiling (DNB).

For PWR operation, DNB heat flux is predicted using the XNB correlation plus correctors for axial heat flux distribution and geometry.

2.1 XNB CORRELATION

The XNB correlation is based upon subchannel analysis of experimental DNB data which was used to determine the effects of local enthalpy, mass velocity, and pressure on DNB heat flux. The analysis of experimental data resulted in the following empirical correlation:

$$Q_{\text{PRED}} = A + B * H_{\text{LOC}} \quad (2.1)$$

where:

$P/P_c = 208.2$ = REDUCED PRESSURE
 G/G_c = REDUCED MASS VELOCITY
 $H_{\text{SUB}} = (H_i - H_{\text{IN}})/906.00$ = REDUCED INLET SUBCOOLING
 Q_{PRED} = PREDICTED CRITICAL HEAT FLUX IN MBTU/HR FT²
 $H_{\text{LOC}} = H/906.00$ = REDUCED LOCAL ENTHALPY
 $G_c = 1.0$ MLB/HR FT²

2.2 NON-UNIFORM AXIAL HEAT FLUX FACTOR

The flux shape factor F developed by Tong et al⁽¹²⁾ provides, in part, an estimate of the effect of non-uniform axial in the prediction of DNB heat flux. This factor is:

$$F = \frac{C \int_0^{l_{crit}} q''(z) [\exp(-C(l_{crit}-Z))] dz}{q''_{loc} [1 - \exp(-C l_{crit})]}$$

where:

C

in^{-1}

q''_{loc} = local heat flux at $Z = l_{crit}$

X_{crit} = local quality at $Z = l_{crit}$

G = mass velocity at $Z = l_{crit}$

The predicted heat flux for a non-uniform axial is

$$QPREDNU = QPRED/FAXIAL \quad (2.4)$$

2.3 GEOMETRIC CORRECTORS

Comparison of data among sets which differed because of bundle length, mixing vanes, or spacer pitch resulted in several multipliers modeling these effects.

2.3.1 Spacer Pitch Factor

The spacer pitch corrector was estimated as a linear fit among data from spacers with pitches ranging from 14.25 inches to 26.2 inches.

(2.5)

where: GAP is the spacer pitch in inches, and
SPC is the multiplier.

Therefore,

(2.6)

2.3.2 Mixing Vane Factor

The mixing vane factor is based upon the spacer pressure drop. Exxon Nuclear ensures hydraulic compatibility with fuels designed by other vendors by measuring pressure drop of full sized fuel bundles. Loss coefficients for spacers are then determined from the pressure drop measurements. The mixing vane factor is:

where:

2.3.3 Length Factor

Finally, a length correction term was observed when comparing all the data from all the bundles. This corrector is:

The estimate for predicted critical heat flux corrected for non-uniform axial, spacer pitch, mixing vanes, and length becomes:

$$QPREDT = QPREDMV * CC. \quad (2.10)$$

2.4 PROCEDURE FOR USING THE XNB CORRELATION AND CORRECTION FACTORS TO PREDICT DNB HEAT FLUX

The following steps are required to predict heat flux to reach boiling transition (DNB) for a subchannel in a bundle with a non-uniform or uniform axial heat distribution.

a) Calculate the local subchannel average cross section values of coolant flow, enthalpy and pressure at each axial node using XCOBRA-IIIC.⁽¹⁾ Appropriate accounting for subchannel mixing in XCOBRA-IIIC is discussed in Section 3.4.1. At each axial node calculate the predicted critical heat flux using Equation (2.1).

b) The F factor is calculated using Equation (2.2) and is then modified by Equation (2.3). The non-uniform axial heat flux is predicted by Equation (2.4).

c) Spacer pitch factor is calculated using Equation (2.5). The predicted heat flux is calculated with Equation (2.6).

d) The mixing vane factor is calculated using Equation (2.7). Equation (2.8) predicts heat flux.

e) The factor accounting for bundle length is calculated using Equation (2.9) and the predicted heat flux is represented by Equation (2.10).

f) The DNBR is determined as the ratio of predicted heat flux to the rod heat flux.

The minimum value of DNBR whether calculated for a test or reactor operation establishes the DNB heat flux for the bundle operation condition being analyzed. For a test or experimental DNB condition, the predicted axial location of DNB determined by the preceding approach may not always coincide with the location of the DNB detection thermocouple giving the first DNB indication during the test. As XNB is able to predict critical heat flux corresponding to the measured critical heat flux such that the MDNBR is acceptable, the precise axial location within the test has no importance.

3.0 COMPARISON OF XNB AGAINST EXPERIMENTAL DNB DATA

Experimental DNB data are compared with predictions of DNB using the XNB correlation. The sources of DNB data include:

- (1) The Exxon Nuclear DNB Test Programs⁽²⁾
 - o Minimum grid data
 - o Non-mixing vane grid data
 - o Mixing vane grid data
- (2) C. Fighetti and D. Reddy⁽³⁾
 - o Non-mixing vane grid data for Combustion Engineering design
 - o Mixing vane grid data of Westinghouse design
- (3) Rosal, et al⁽¹⁴⁾
 - o Non-mixing vane grid data
 - o Mixing vane grid data

3.1 EXXON NUCLEAR PWR DNB TEST DATA

The Exxon Nuclear DNB test programs were conducted in the high pressure heat transfer facility at the Chemical Engineering Research Laboratories of Columbia University.

The test programs^(4,5,6,7) used test assemblies of 5x5 arrays. Characteristics of these arrays along with operating test parameter ranges are presented in Table 3.1.

3.1.1 Test Sections ENC-1 & 2

Two test sections, each with 25 rods of six foot length and uniform axial and radial profiles are included in this analysis. The characteristics of the test sections and range of experimental conditions are shown on Table 3.1.

The distinction between the sections was the grid design. ENC-1 used a simple support grid, referred to as a minimum grid because of the minimum impact the grid has on the flow. ENC-2 used a non-mixing vane grid prototypic of production grids. The rod arrangements for the two designs are shown as Figure 3.1. Figures 3.2 and 3.3 show locations of grid spacers while a comparison of measured to predicted heat flux is illustrated on Figures 3.4 and 3.5. The mean value of DNBR was 1.029 with a standard deviation of 0.1186 for ENC-1 data and 0.983 with a standard deviation of 0.1084 for the ENC-2 data.

3.1.2 Test Sections ENC-3 & 4

Two test sections, each with 21 heated rods of six foot length uniform axial and non-uniform radial profiles are included in this analysis. The characteristics of the test sections and range of experimental conditions are shown on Table 3.1. The mixing vane density was the distinguishing feature between the designs. ENC-4 used twice the number of mixing vanes as ENC-3.

The rod arrangements, grid locations, and comparison of measured to predicted heat flux are shown on Figures 3.6 through 3.9. The mean MDNBR was 0.939 with a standard deviation of 0.0895 for ENC-3 and was 0.985 with a standard deviation of 0.1196 for ENC-4.

3.1.3 Test Section ENC-5

This test incorporated a mixing vane spacer design with a 26-inch spacer pitch. The characteristics of the test section and range of experimental conditions are shown on Table 3.1. The rod arrangement, grid location, and the comparison of measured to predicted heat flux are shown on Figures 3.10 through 3.12. The mean MDNBR was 0.915 with a standard deviation of 0.843.

3.1.4 Test Section ENC-6

This section represented a configuration typical of a 17x17 array with 0.360 diameter fuel. Twenty-four (24) heated rods and one unheated ceramic simulated guide tube were tested. The outside diameter of the heated rods was constant while the inside diameter was tapered to achieve a non-uniform axial heat flux.

Characteristics of the test section and experimental conditions are shown on Table 3.1. Rod arrangement, grid location, thermocouple location, axial profile, and comparison between predicted and measured heat flux are shown on Figures 3.13 through 3.16. The mean MDNBR was 0.995 with a standard deviation of 0.0749.

3.2 C. FIGHETTI AND D. REDDY DNB DATA

The experimental tests were conducted in the high pressure heat transfer facility at the Columbia Engineering Research Laboratories of Columbia University.

The data reported by Fighetti and Reddy⁽³⁾ includes results from major nuclear fuel vendors throughout the world. Several sections selected for analysis below included test sections using prototypic spacers and geometry of Combustion Engineering fuel design and test sections with spacers and geometry prototypic of Westinghouse fuel design.

3.2.1 Combustion Engineering DNB Test Data

Two test sections, each with 21 heated rods of 0.382 inch diameter are included in this analysis. Characteristics of the test sections and the experimental range of operating conditions are shown on Table 3.1. One test section used a uniform axial while the other was a non-uniform sinusoidal axial power profile. The rod arrangement for test section CE-47 is shown in Figure 3.17 while that for CE-59 is shown in Figure 3.18. The location of grid spacers (all non-mixing vane) and thermocouples are shown on Figure 3.19 while the non-uniform axial profile for CE-59 is shown on Figure 3.20. Comparison of measured to predicted heat flux values are shown on Figures 3.21 and 3.22 for CE-47 and CE-59, respectively. The mean value of the ratio of predicted to measured heat flux for CE-47 was 1.028 with a standard deviation of 0.0741 while the mean for CE-59 was 1.023 with a standard deviation of 0.0820.

3.2.2 Westinghouse DNB Test Data

Two test sections with 24 and 25 heated rods of 0.374 inch diameter are shown in Figures 3.23 and 3.24. The spacer location and thermocouple locations are shown in Figure 3.25 while the non-uniform sinusoidal axial profile is shown in Figure 3.26. Test section characteristics and experimental range of conditions are shown in Table 3.1. XNB predicted the critical heat flux over the range of conditions shown in Table 3.1. The mean DNBR for WH-162 was 0.992 while its standard deviation is 0.0845. For test section WH-164, the mean is 0.950 with a standard deviation of 0.067. The predicted heat flux to measured heat flux is illustrated in Figures 3.27 and 3.28 for WH-162 and WH-164, respectively.

3.3 ROSAL, ET AL TEST SECTIONS⁽¹⁴⁾

Four test sections of eight foot length are represented in this analysis. Rosal-4 represents a section in which the grids have no mixing vanes. Rosal-8 differs from Rosal-2 principally because of spacer pitch. Test section characteristics and operation conditions are shown on Table 3.1. Rod layout, grid location, and axial profiles are shown on Figures 3.29 through 3.31. Comparisons of measured to predicted heat flux is shown on Figures 3.32 through 3.35. Mean DNBR's were 0.976, 0.933, 0.970, 1.001 with standard deviation of 0.1118, 0.1043, 0.0987 for sections Rosal-2, Rosal-4, Rosal-7, and Rosal-8, respectively.

3.4 DISCUSSION AND CONCLUSIONS OF ANALYSIS OF DNB TEST DATA

The method to predict DNB heat flux described in Section 2.0 was used in the analysis of the data discussed in Section 3.0. The DNB prediction used a subchannel code to evaluate local flow conditions which are required as input to the Equations (2.1) through (2.10). These equations correspond to the XNB correlation plus corrections for effects of non-uniform axial power distribution and geometric parameters. Table 3.2 summarizes key statistical results for each section and overall.

3.4.1 Subchannel Mixing

Grid spacers promote subchannel mixing which reduces subchannel to subchannel enthalph gradients and tends to sweep vapor layers from the rod surface. This increases the DNB heat flux for a given set of fluid conditions.

Depending on grid design, subchannel mixing can be a combination of forced diversion mixing and turbulent mixing. In the analysis of the data presented in this document, the calculation of mixing included flow diversion mixing (due to subchannel static pressure differences caused by grid spacer pressure losses) and turbulent mixing. Forced diversion mixing was not included in the analysis. All subchannels of a given test section used the same grid spacer loss coefficient which corresponded to experimentally determined loss coefficients on grid spacers similar to those used in the test. The turbulent mixing parameters used in the analysis of the DNB data were:

where the basic turbulent mixing equation is:

$$W = \beta sG$$

where:

- β = turbulent mixing parameter
- s = rod-to-rod spacing
- D = subchannel hydraulic diameter
- G = subchannel mass velocity
- W = turbulent cross flow

These values of $\beta s/D$ are based on experimental data⁽⁹⁾ from a variety of fuel designs; Reference (9) verifies the above mixing relations to these data.

Table 3.1 Summary of Test Conditions

<u>Test Section</u>	<u>ENC-1</u>	<u>ENC-2</u>	<u>ENC-3</u>	<u>ENC-4</u>	<u>ENC-5</u>
Heated Length (ft)	6	6	6	6	5.5
Axial Heat Flux Distribution	UNIFORM	UNIFORM	UNIFORM	UNIFORM	UNIFORM
Radial Power Distribution	UNIFORM	UNIFORM	.95-1.10	.95-1.10	.95-1.08
Grid Design	MG	NV	MV	MV	MV
Hydraulic Diameter, Nominal Channel, inch	.520	.520	.514	.514	.528
Rod O.D., inch	.413	.413	.421	.421	.424
Grid Spacing, inch	15.5	15.5	15.7	15.7	26.2
KLOSS**					
Range of Experimental Parameters					
Pressure, psia	1500-2160	1500-2155	1500-2260	1500-2270	1745-2265
Inlet Temperature, °F	460-620	470-620	420-630	420-630	400-620
Inlet Avg. Mass Velocity, Mlb/hr-ft ²	1.0-2.56	1.00-2.53	1.0-2.77	1.0-2.72	.98-2.75
Number of Data Points	28	24	73	80	59

* Mixing vane grids were on 22-inch pitch.
Simple support grids were halfway between MV grids.

**

Table 3.1 Summary of Test Conditions (Continued)

<u>Test Section</u>	<u>ENC-6</u>	<u>CE-47</u>	<u>CE-59</u>	<u>WH-162</u>	<u>WH-164</u>
Heated Length (ft)	12	12.5	12.5	14	14
Axial Heat Flux Distribution	COSU	UNIFORM	COSU	COSU	COSU
Radial Power Distribution	.97-1.10	.97-1.14	.96-1.20	.95-1.10	.94-1.10
Grid Design	MV	NV	NV	MV	MV
Hydraulic Diameter, Nominal Channel, inch	0.5101	0.4714	0.4714	0.4635	0.4635
Rod O.D., inch	0.360	0.382	0.382	0.374	0.374
Grid Spacing, inch	20.56	14.30	14.30	22.0/11.0*	22.0/11.0*
KLUSS					
Range of Experimental Parameters					
Pressure, psia	1600-2400	1395-2405	1495-2415	1500-2425	1500-2425
Inlet Temperature, °F	445-615	362-631	333-626	429-610	384-606
Inlet Avg. Mass Velocity, Mlb/hr-ft ²	0.9-3.1	0.9-4.0	0.9-4.0	0.9-3.1	0.9-3.1
Number of Data Points	62	96	89	53	53

* Mixing vane grids were on 22-inch pitch.

Simple support grids were halfway between MV grids.

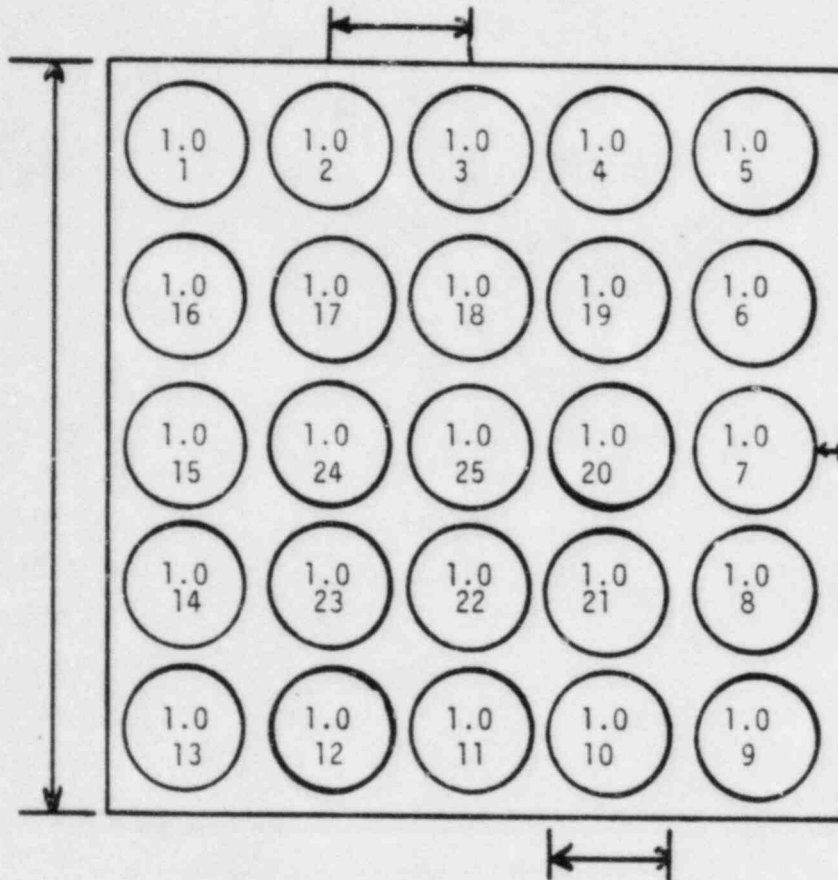
Table 3.1 Summary of Test Conditions (Continued)

<u>Test Section</u>	<u>Rosal-2</u>	<u>Rosal-7</u>	<u>Rosal-4</u>	<u>Rosal-8</u>
Heated Length (ft)	8	14	8	8
Axial Heat Flux Distribution	U SINE U	COSU	U SINE U	COSU
Radial Power Distribution				
No. Inner Rods - % Power	4-100%	4-100%	4-100%	4-100%
No. Outer Rods - % Power	12-83.1%	12-94%	12-83%	12-94%
Grid Design	grids w/MV	grids w/MV	grids w/o MV	grids w/MV
Hydraulic Diameter, Nominal Channel, inch	0.507	0.507	0.507	0.507
Rod O.D., inch	0.422	0.422	0.422	0.422
Grid Spacing, inch	20*	20*	20*	26*
KLOSS				
Range of Experimental Parameters				
Pressure, psia	1504-2410	1491-2105	1492-2148	1490-2432
Inlet Temperature, °F	466-627	479-580	481.5-603	478-626
Inlet Avg. Mass Velocity, Mlb/hr-ft ²	2.02-3.58	2.07-3.63	1.50-3.62	2.02-3.61
Number of Data Points	28	11	26	32

* Simple grid between indicated grid spacer.

Table 3.2 Statistical Summary

<u>Test Section</u>	<u>Number</u>	<u>Mean</u>	<u>Standard Deviation</u>
CE-47	96	1.028	0.0741
CE-59	89	1.023	0.0820
WH-64	53	0.950	0.0677
WH-62	53	0.992	0.0845
ENC-6	62	0.995	0.0749
ROSAL-2	28	0.976	0.1118
ROSAL-4	26	0.933	0.0843
ROSAL-7	11	0.970	0.1043
ROSAL-8	32	1.001	0.0987
ENC-1	28	1.029	0.1186
ENC-2	24	0.983	0.1084
ENC-3	73	0.939	0.0895
ENC-4	80	0.985	0.1196
ENC-5	59	0.915	0.0843
TOTAL	714	0.984	0.0964



LOWER ROD NUMBER PROVIDES ROD NUMBER SPECIFIED
IN DATA AS THE ROD INDICATING CHF

Figure 3.1 Test Assembly Geometry and Local
Power Distribution for ENC 1 & 2
Test Assemblies

Figure 3.2 Spacer, Pressure Tap, and Thermocouple Locations
for ENC 1 Test

Figure 3.3 Spacer, Pressure Tap and Thermocouple Locations
for ENC 2 Test

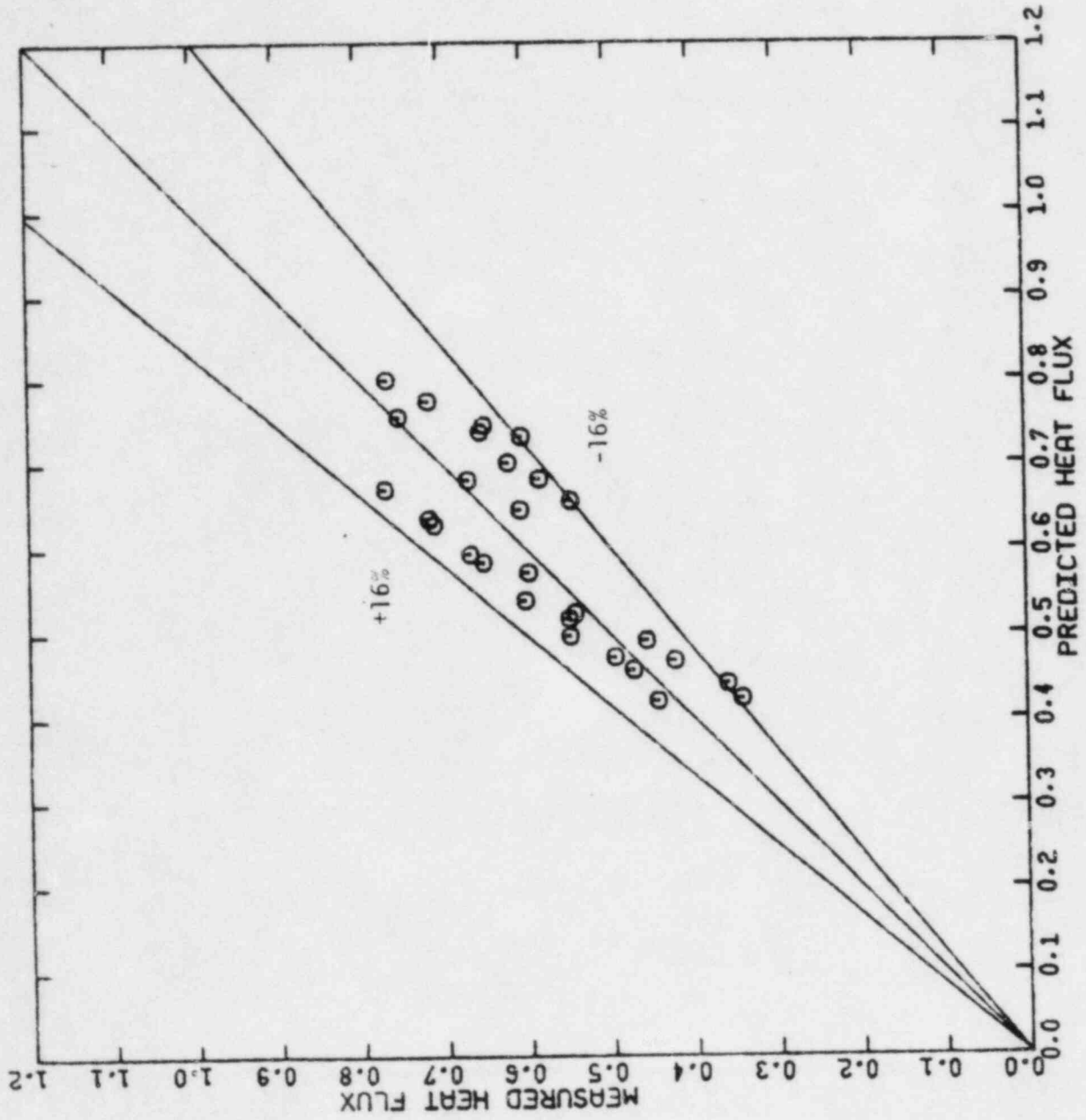


FIGURE 3.4 COMPARISON OF HEAT FLUX - ENC.1

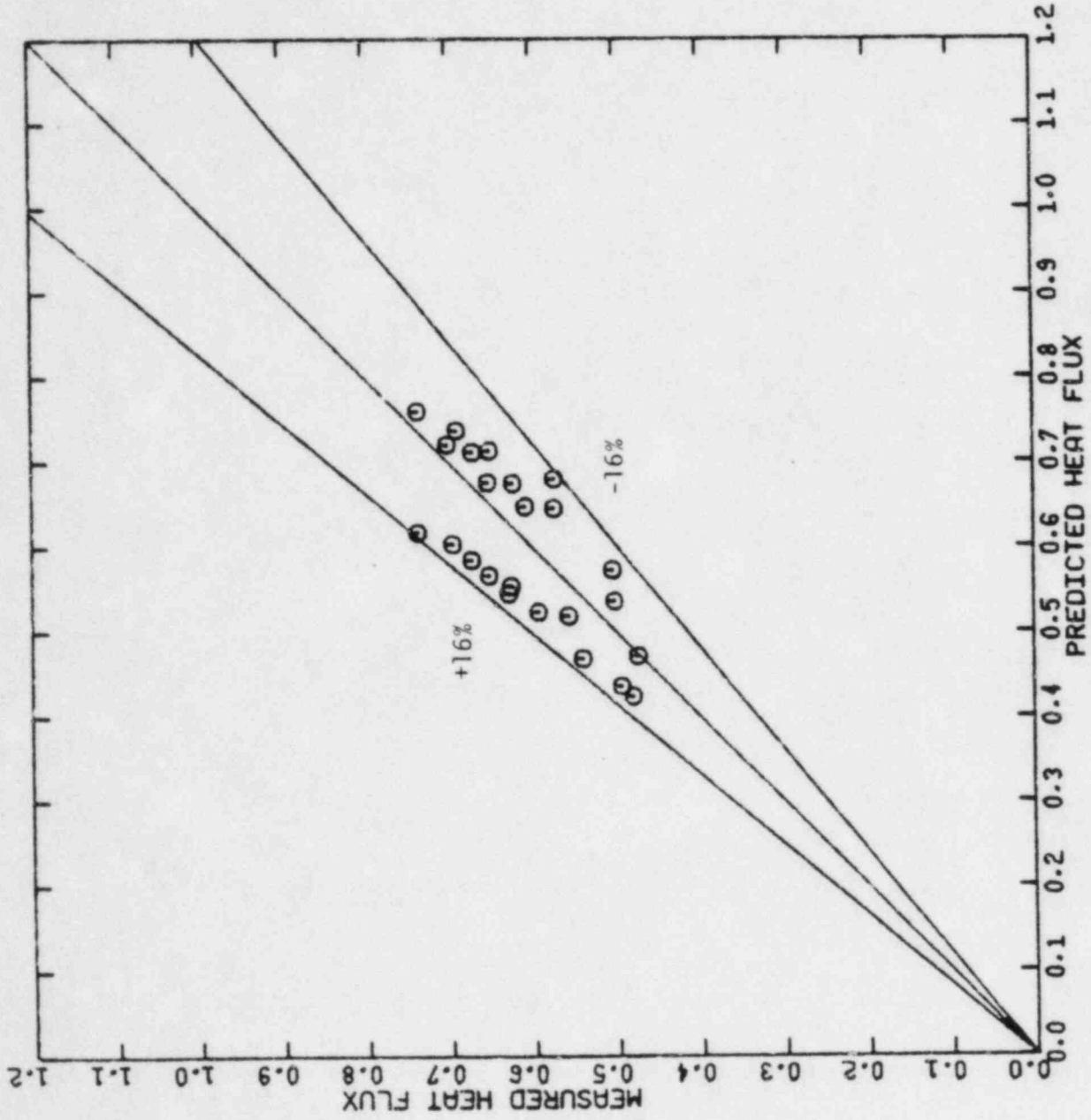
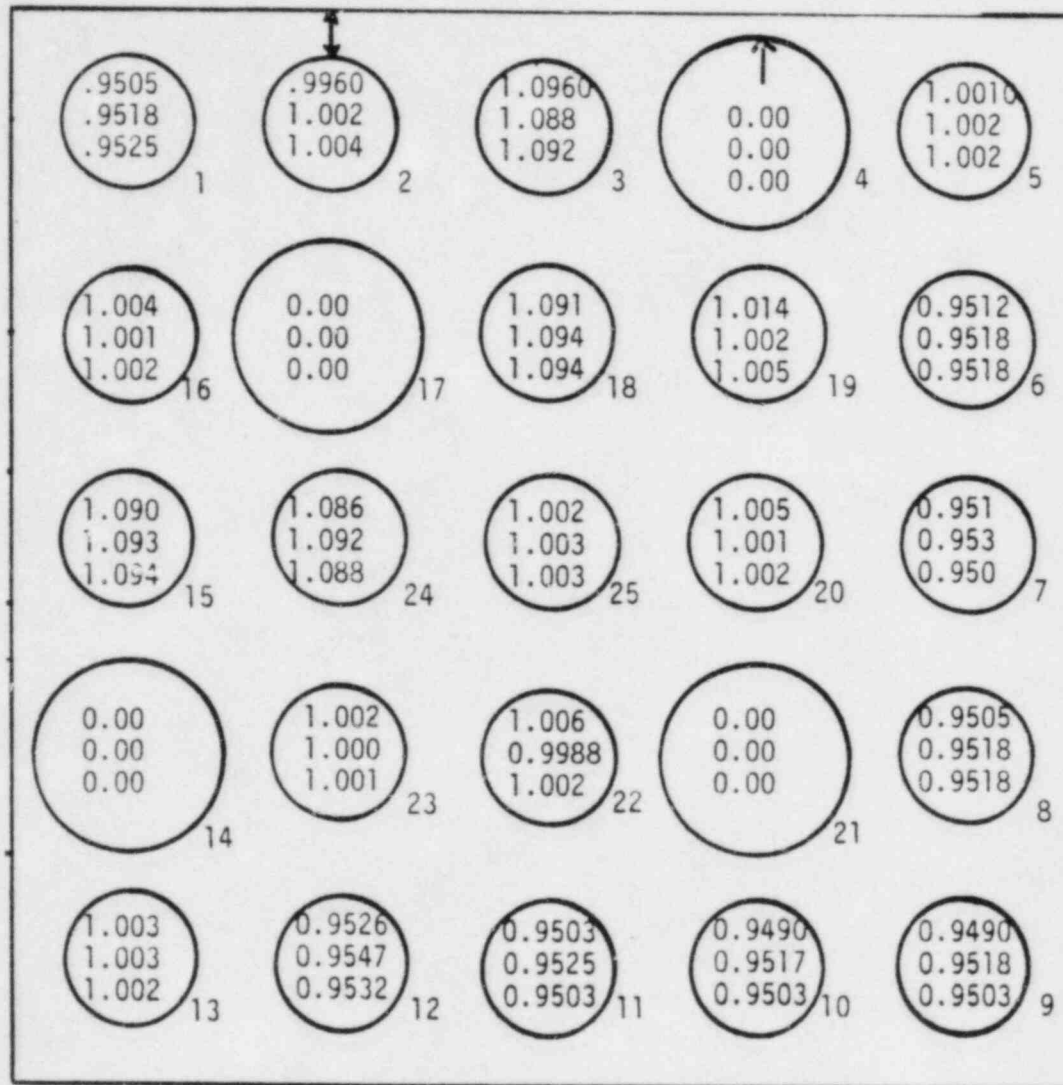


FIGURE 3.5 COMPARISON OF HEAT FLUX - ENC.2

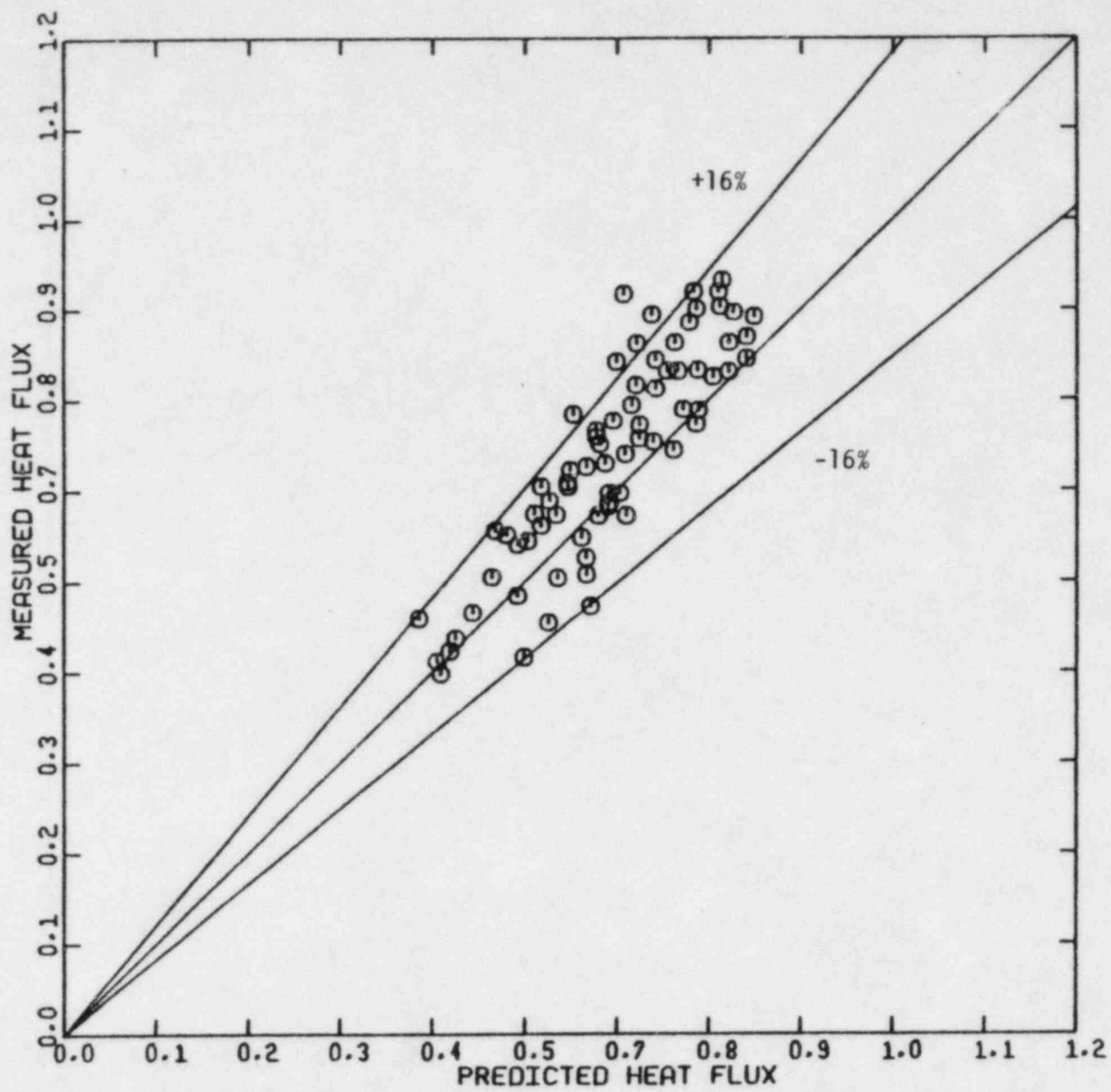


TOP: TEST 1
MIDDLE: TEST 2-1
BOTTOM: TEST 2-2

NUMBER OUTSIDE SHOWS ROD NUMBER

Figure 3.6 Test Assembly Geometry and Local Power Distribution for ENC 3 & 4 Test Assemblies

Figure 3.7 Spacer, Pressure Tap and Thermocouple
Locations for Tests ENC 3 & 4



3-19

XN-NF-621 (NP)(A)
Revision 1

FIGURE 3.8 COMPARISON OF HEAT FLUX - ENC-3

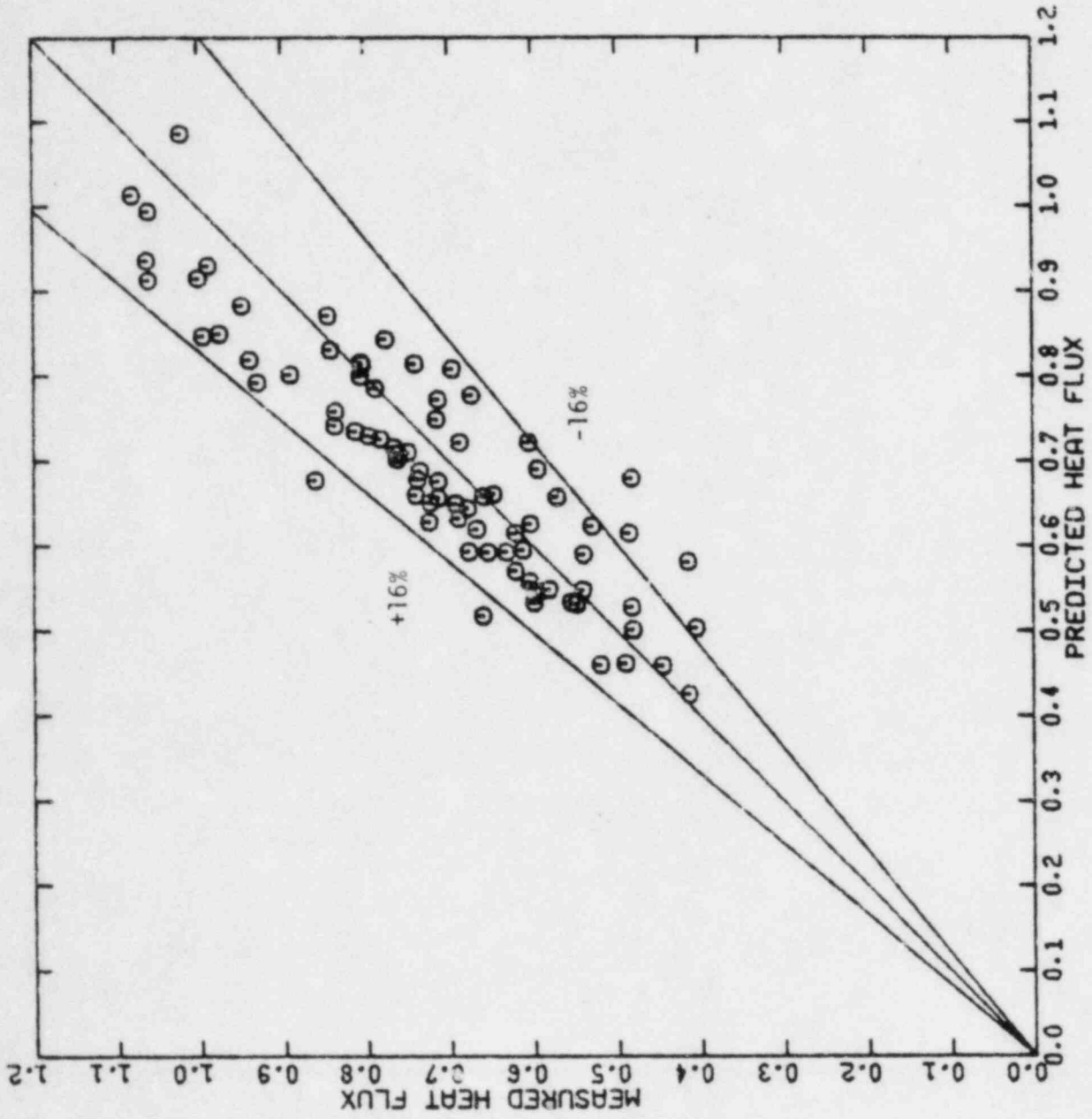
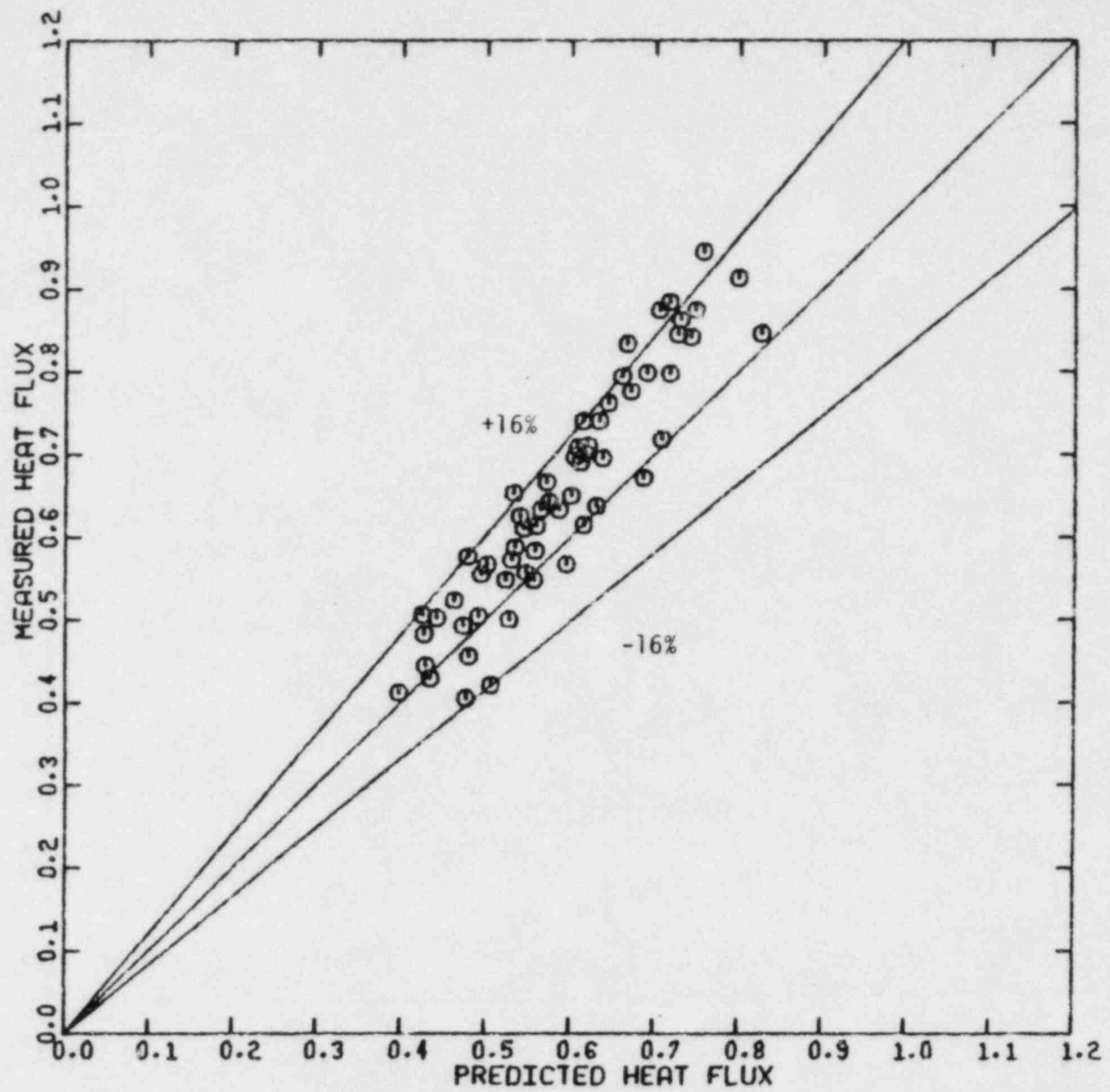


FIGURE 3.9 COMPARISON OF HEAT FLUX - ENC.4

NUMBER OUTSIDE SHOWS ROD NUMBER

Figure 3.10 Test Assembly Geometry and Local Power
Distribution for ENC 5 Test Assembly

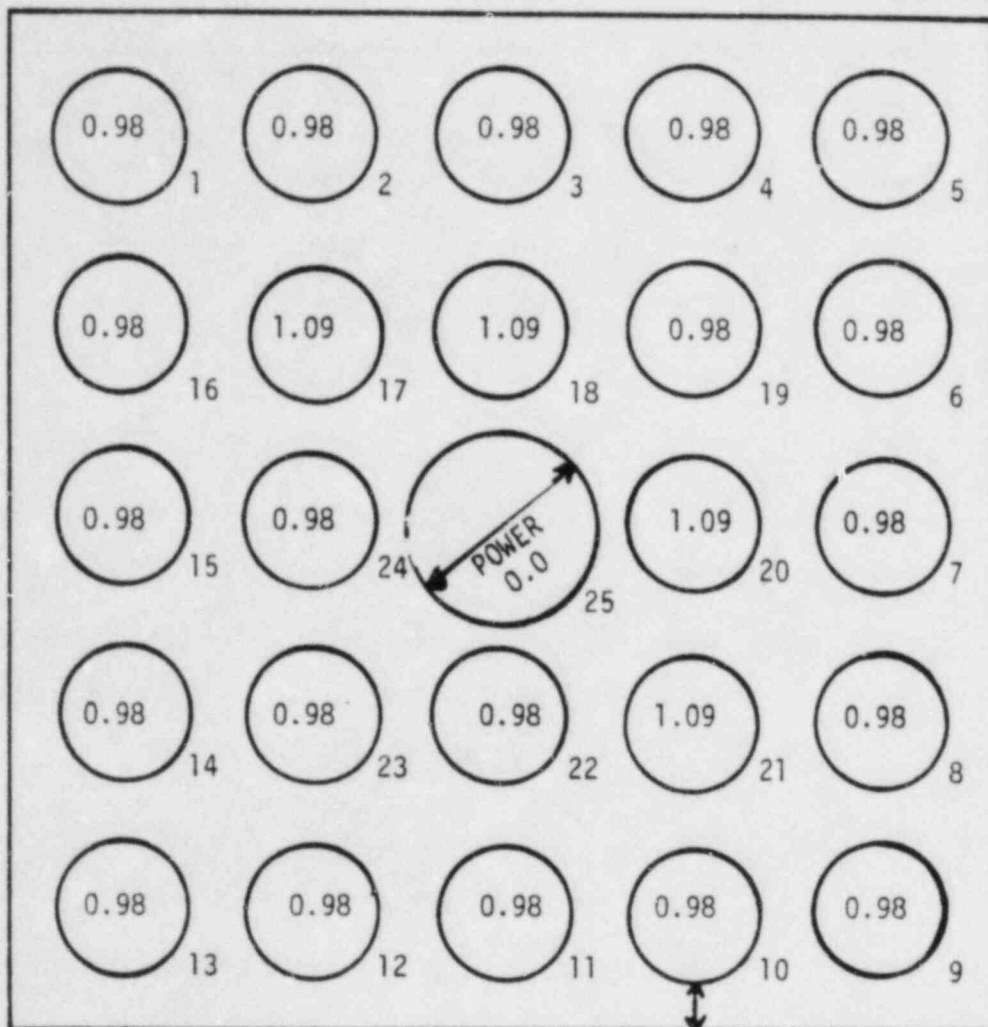
Figure 3.11 Spacer, Pressure Tap and Thermocouple
Locations for ENC 5 Test Assembly



3-23

XN-NF-621 (NP)(A)
Revision 1

FIGURE 3.12 COMPARISON OF HEAT FLUX - ENC. 5



NUMBER OUTSIDE SHOWS ROD NUMBER

Figure 3.13 Test Assembly Geometry and Local Power Distribution for ENC 6 Test Assembly

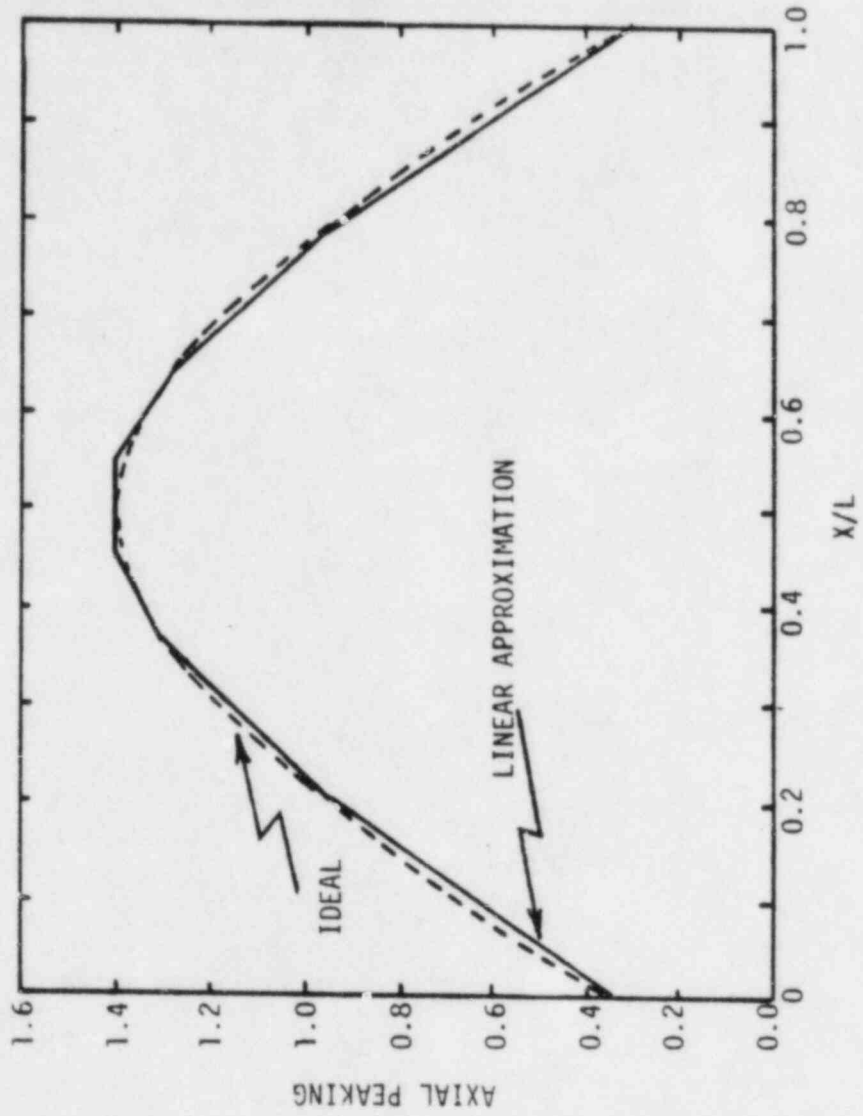


Figure 3.14 Axial Power Distribution for ENC 6 Test Section

Figure 3.15 Spacer, Pressure Tap and Thermocouple
Location for ENC 6 Test Assembly

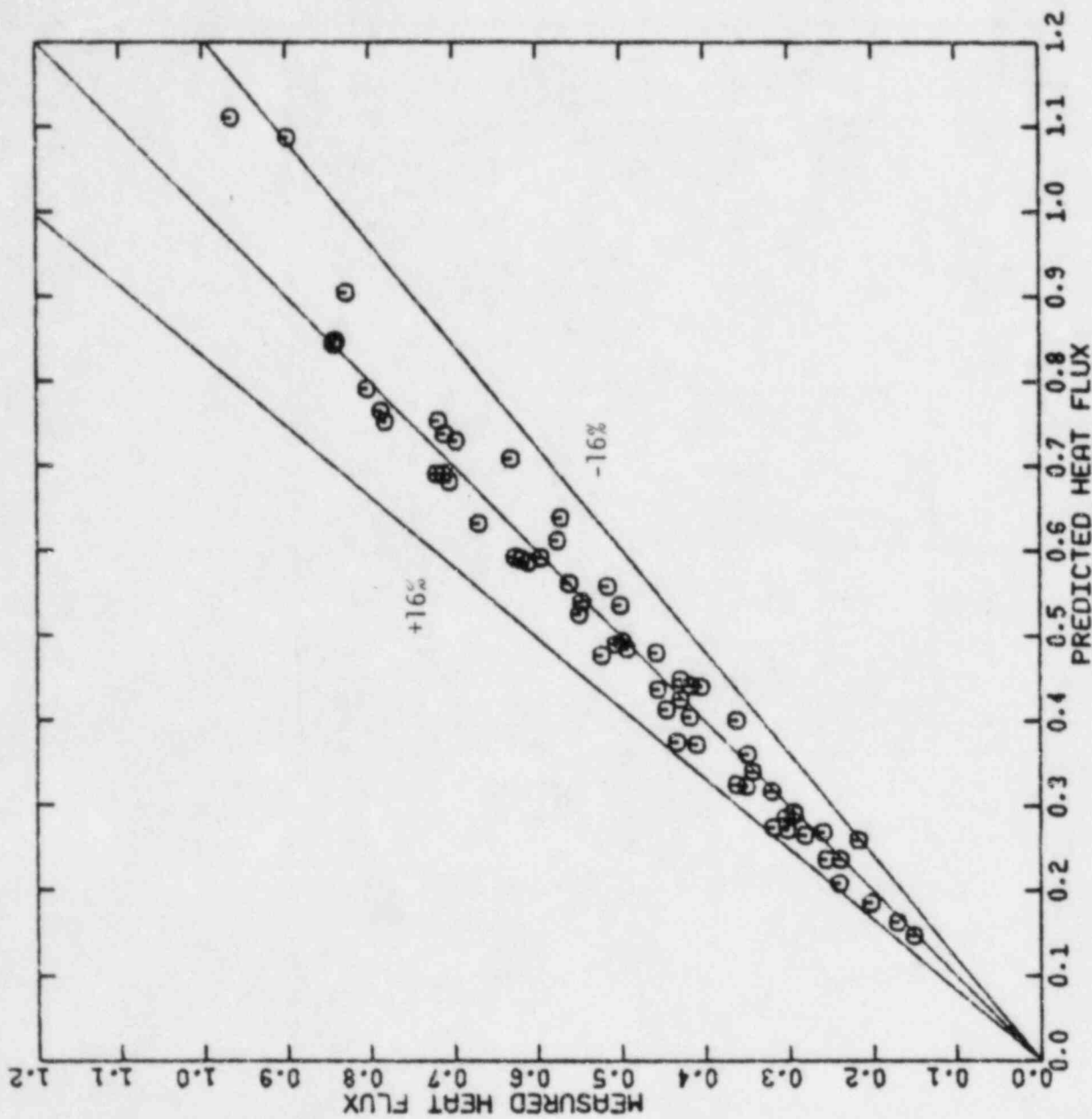
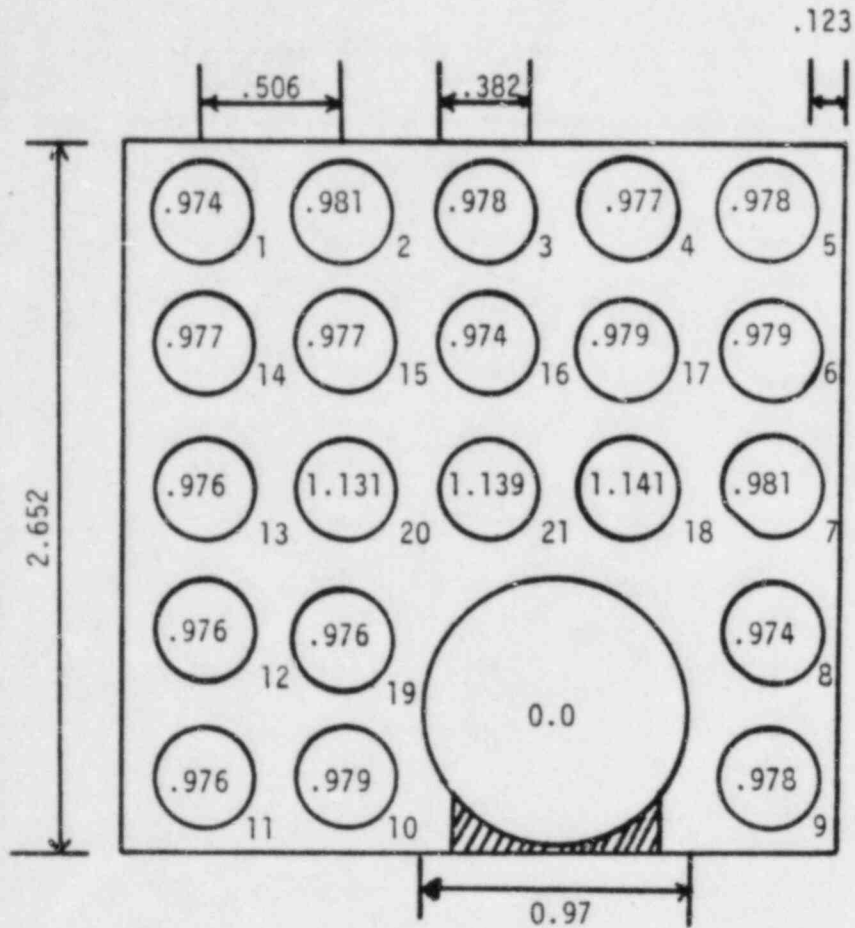
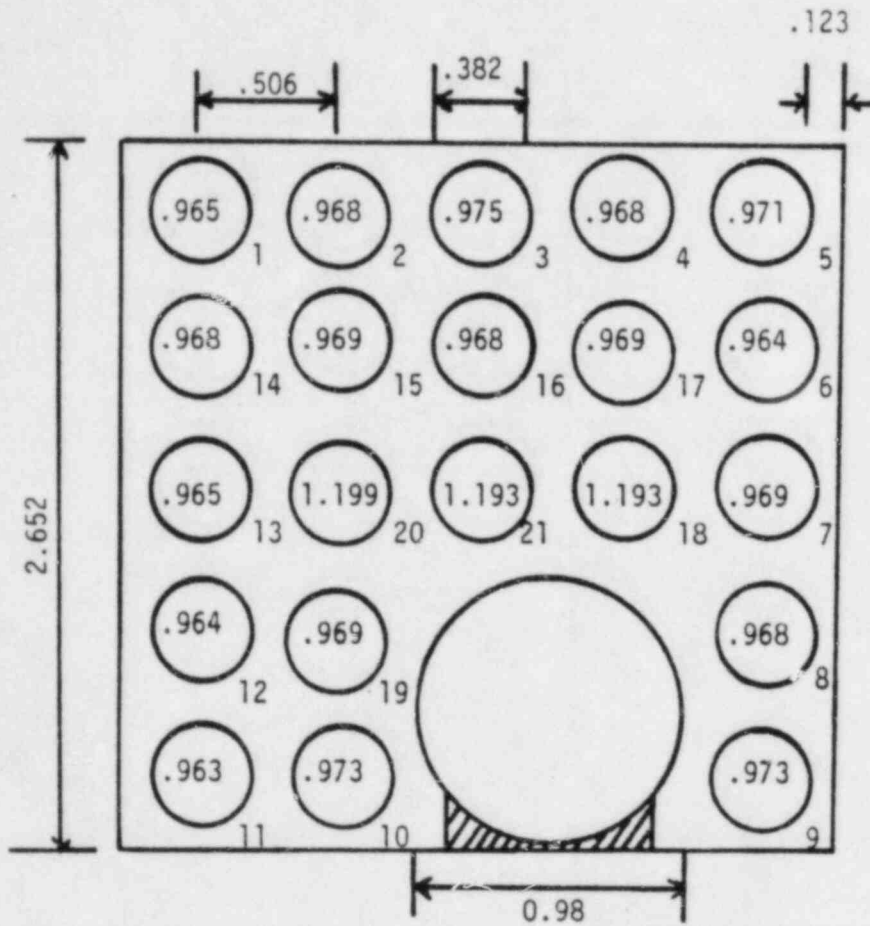


FIGURE 3.16 COMPARISON OF HEAT FLUX - ENC.6



NUMBER OUTSIDE SHOWS ROD NUMBER

Figure 3.17 Test Assembly Geometry and Local Power Distribution For CE-47 Test Section



NUMBER OUTSIDE SHOWS ROD NUMBER

Figure 3.18 Test Assembly Geometry and Local Power Distribution For CE-59 Test Section

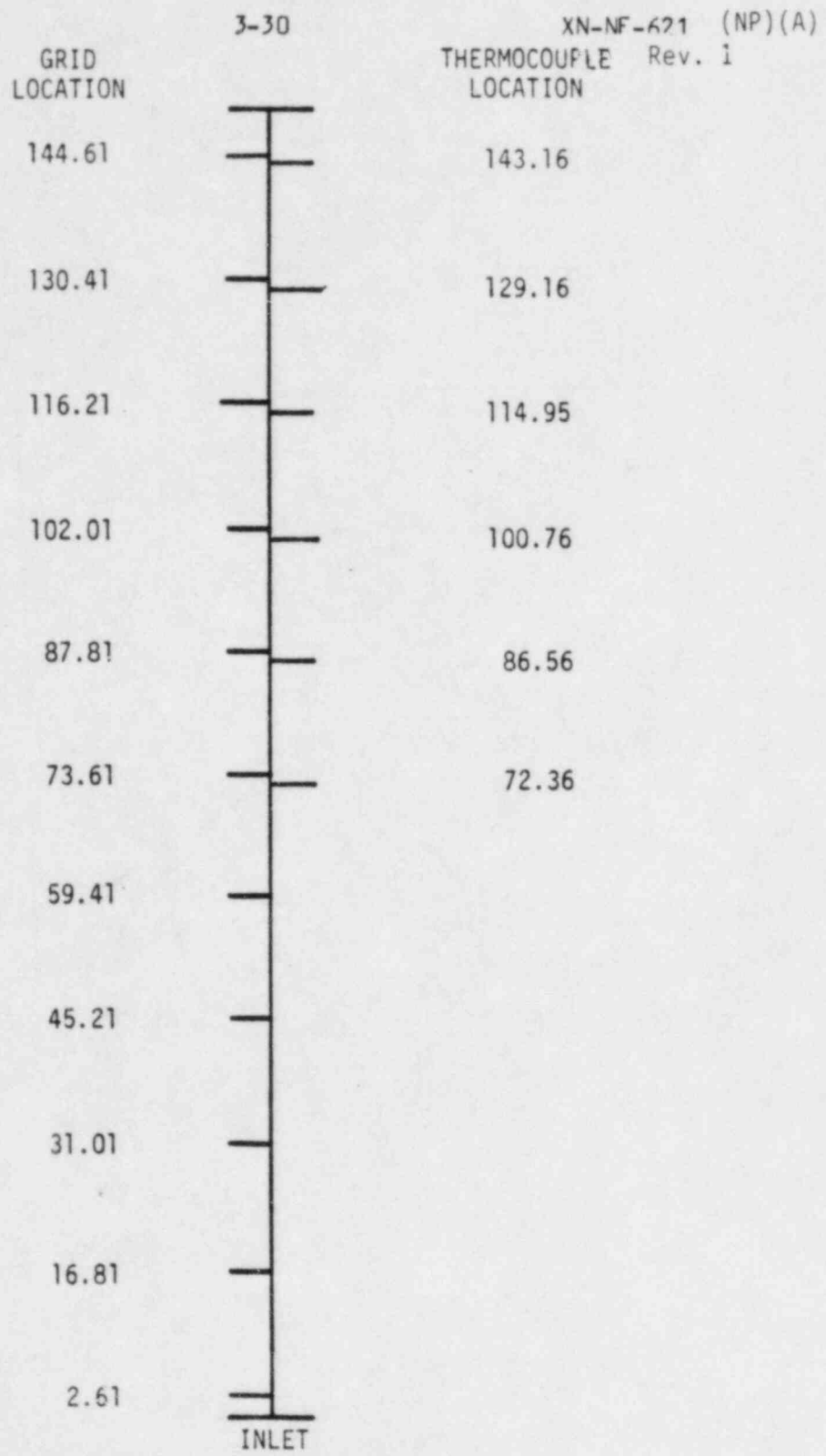


Figure 3.19 Spacer and Thermocouple Locations For CE-59 Test Section and Spacer Locations For CE-47 Test Section

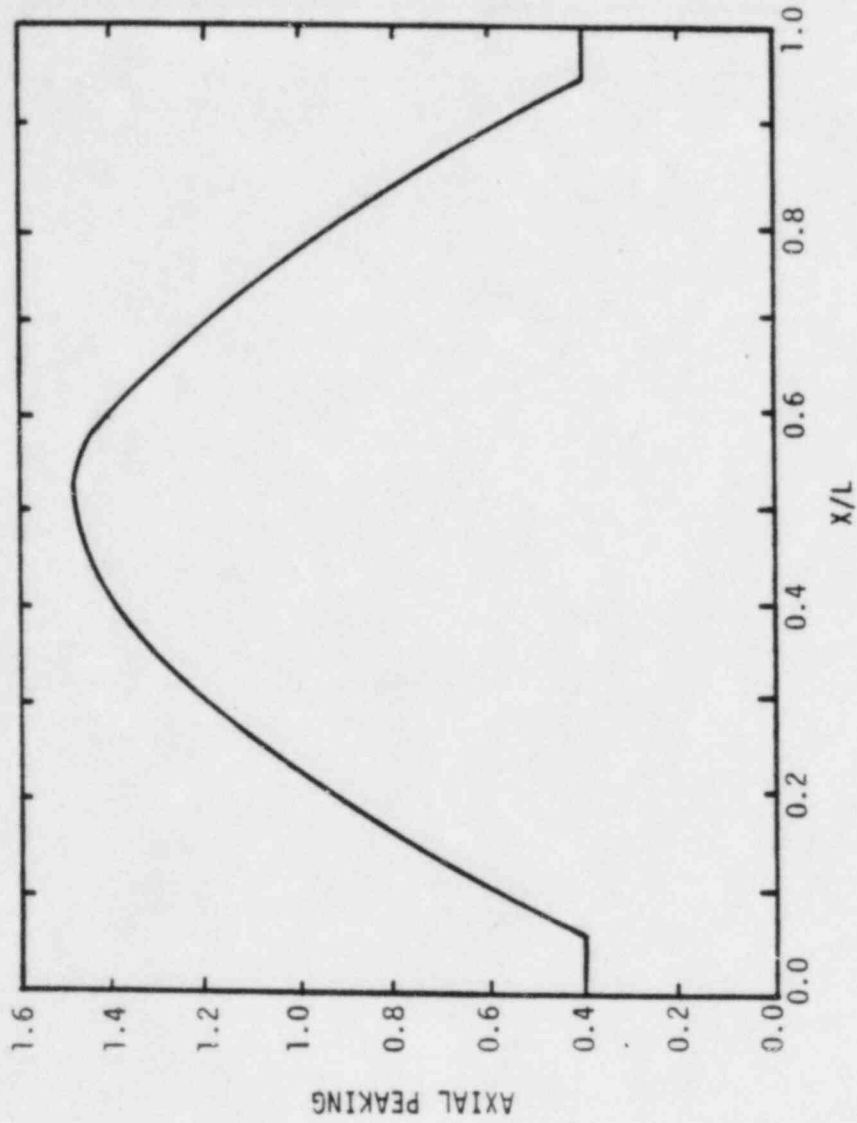


Figure 3.20 Axial Power Distribution For CE-59
Test Section

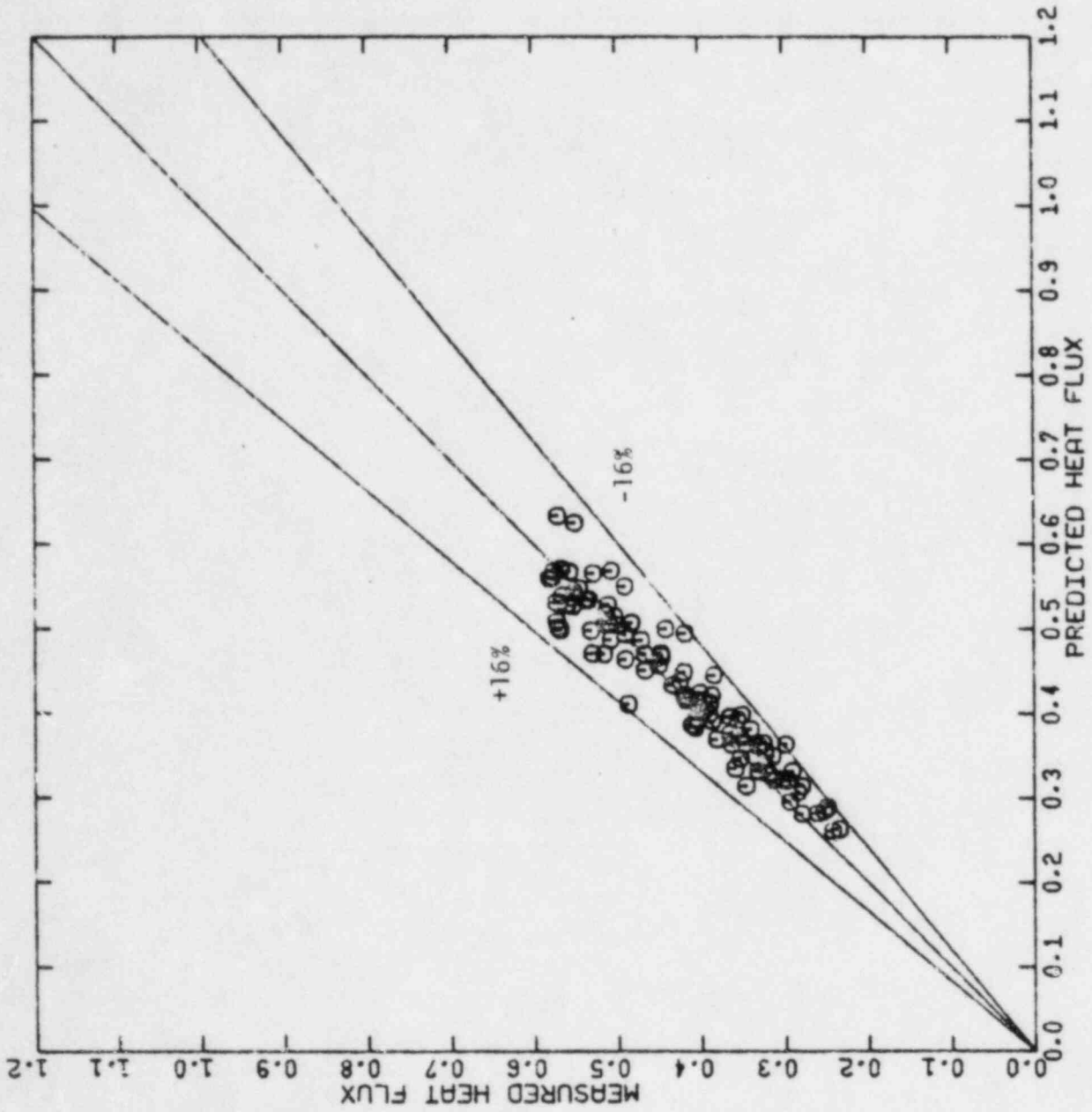
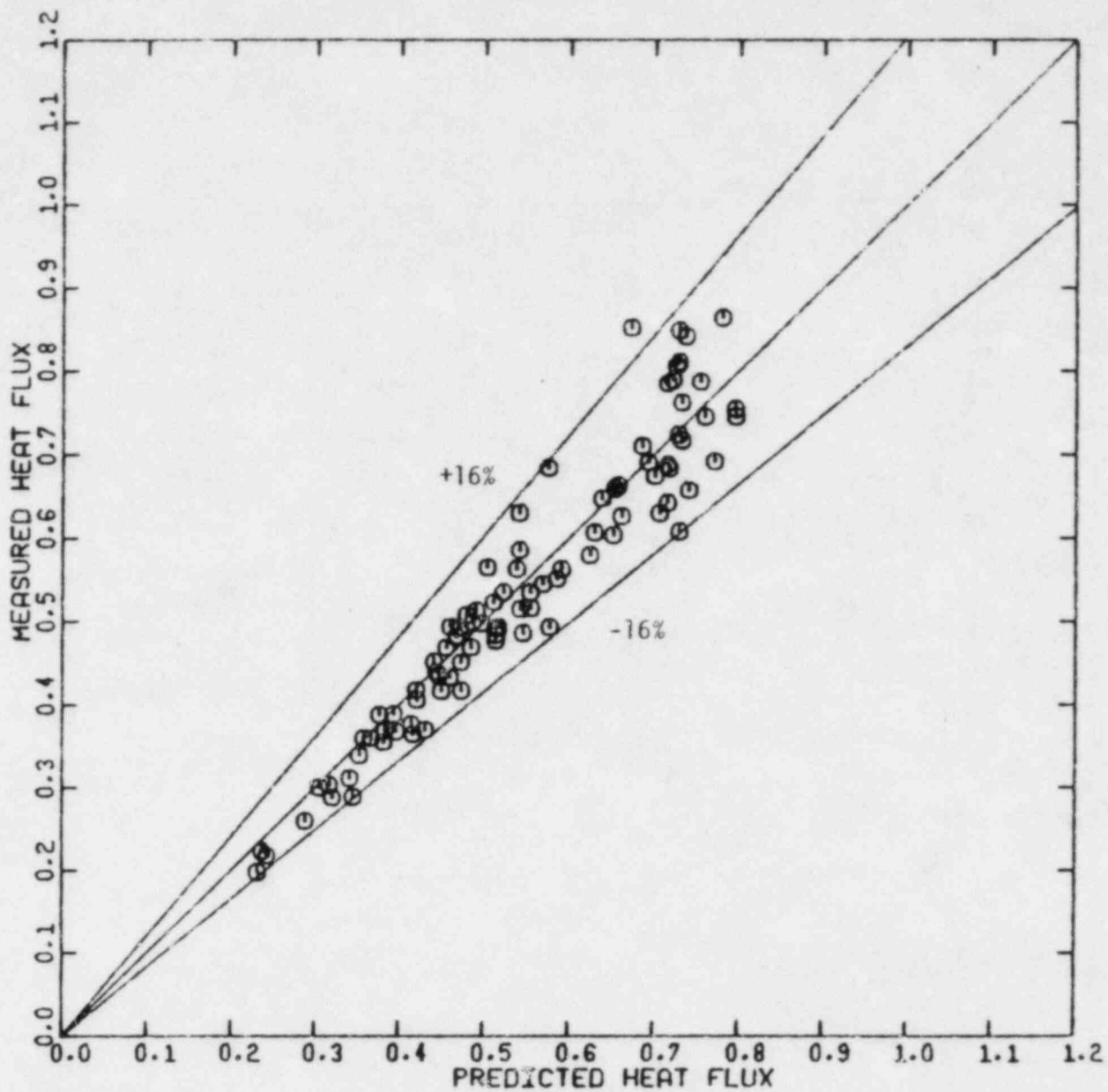


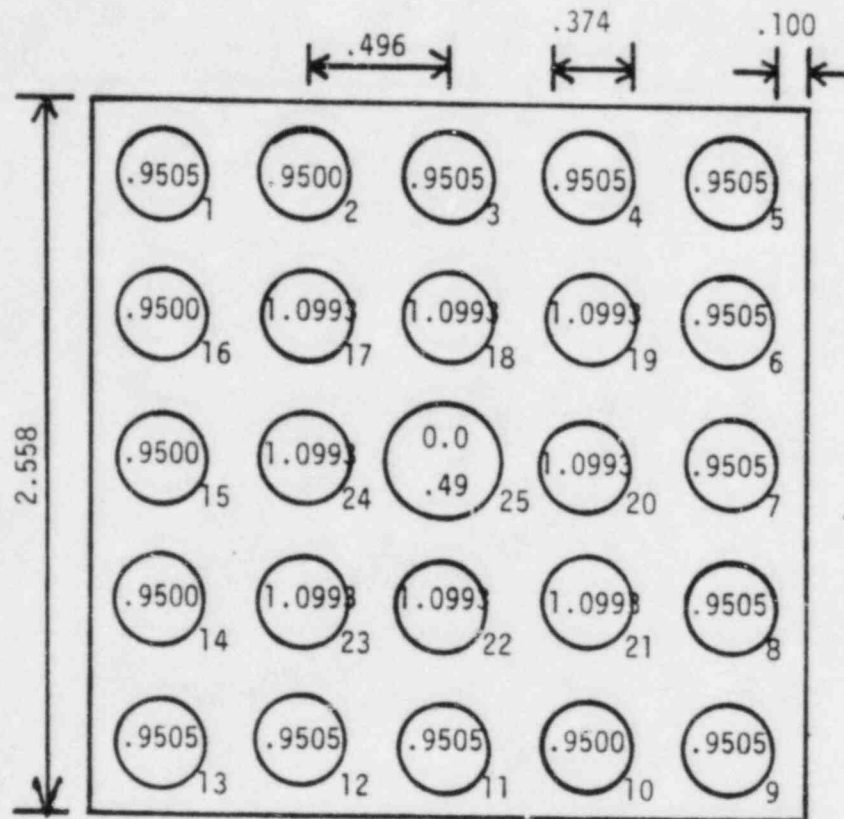
FIGURE 3.21 COMPARISON OF HEAT FLUX - CE47



3-33

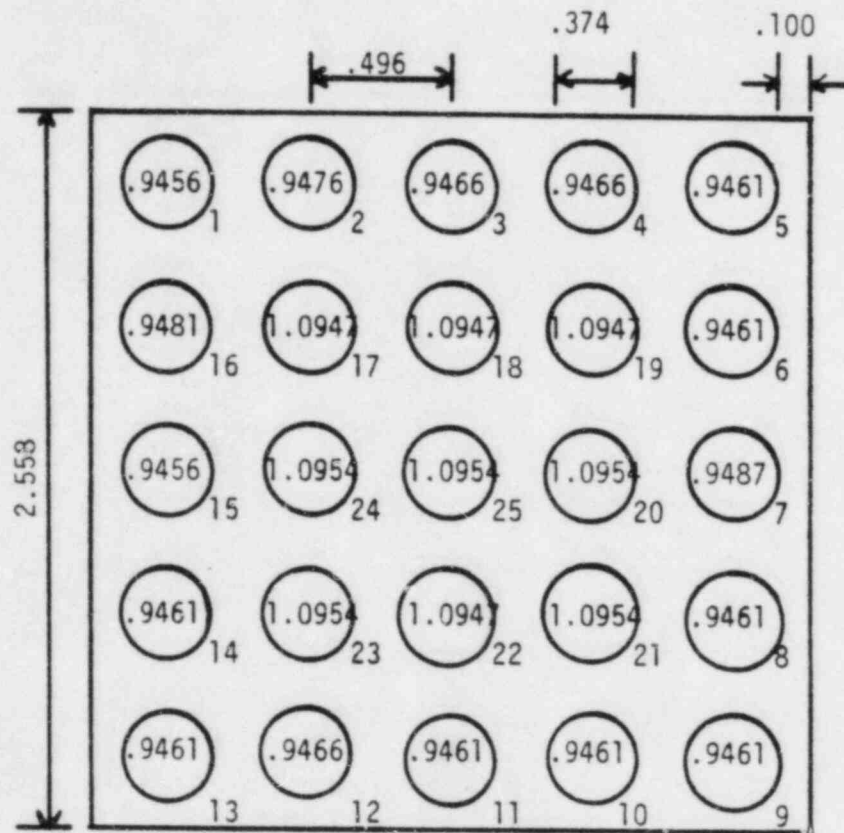
XN-NF-621 (NP)(A)
Revision 1

FIGURE 3.22 COMPARISON OF HEAT FLUX - CE59



NUMBER OUTSIDE SHOWS ROD NUMBER

Figure 3.23 Test Assembly Geometry and Local Power Distribution For W-162 Test Section



NUMBER OUTSIDE SHOWS ROD NUMBER

Figure 3.24 Test Assembly Geometry and Local Power Distribution for W-164 Test Section

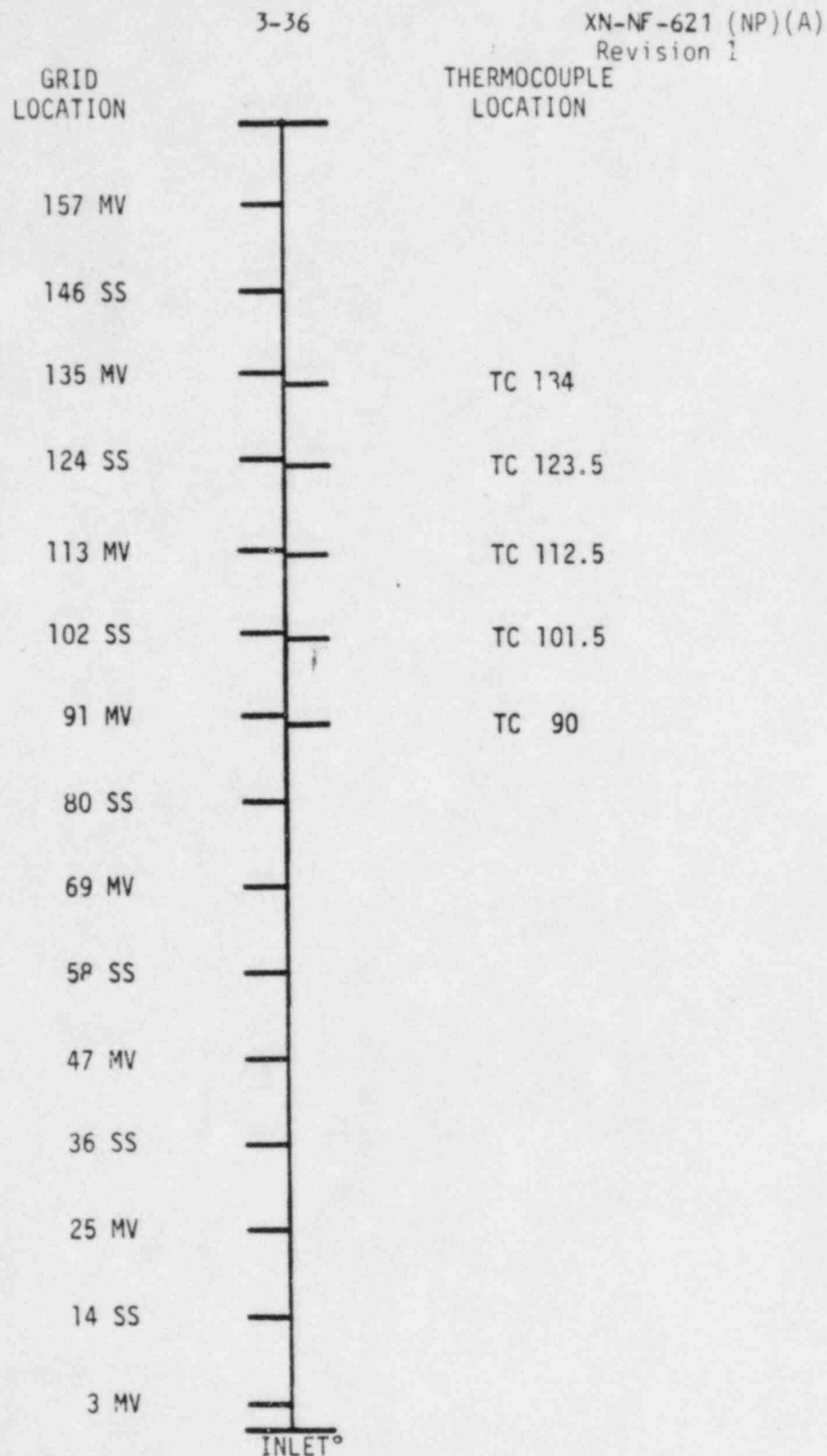


Figure 3.25 Spacer and Thermocouple Locations for Test Sections W-162 and W-164; MV = Mixing Vane Grid; SS = Simple Support and TC = Thermocouple. Distances From Start of Heated Length.

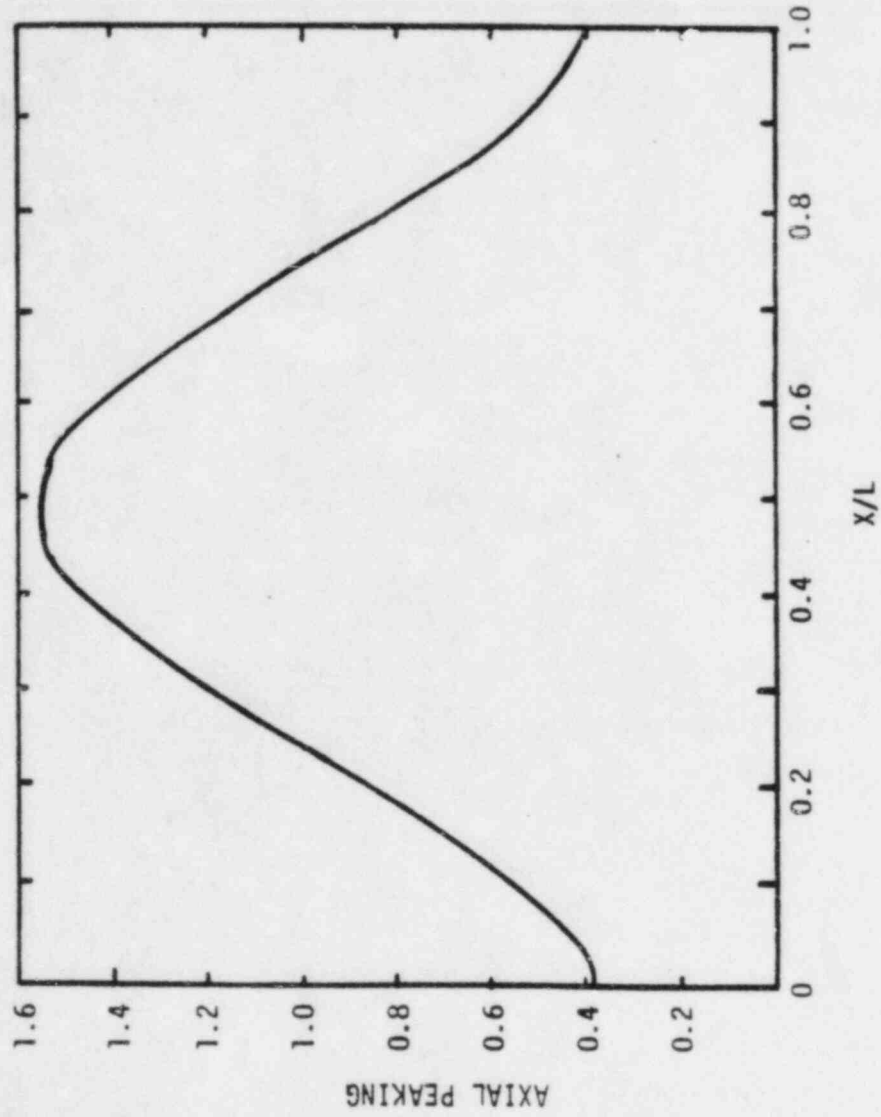


Figure 3.26 Axial Power Distribution for W-162 and W-164 Test Sections

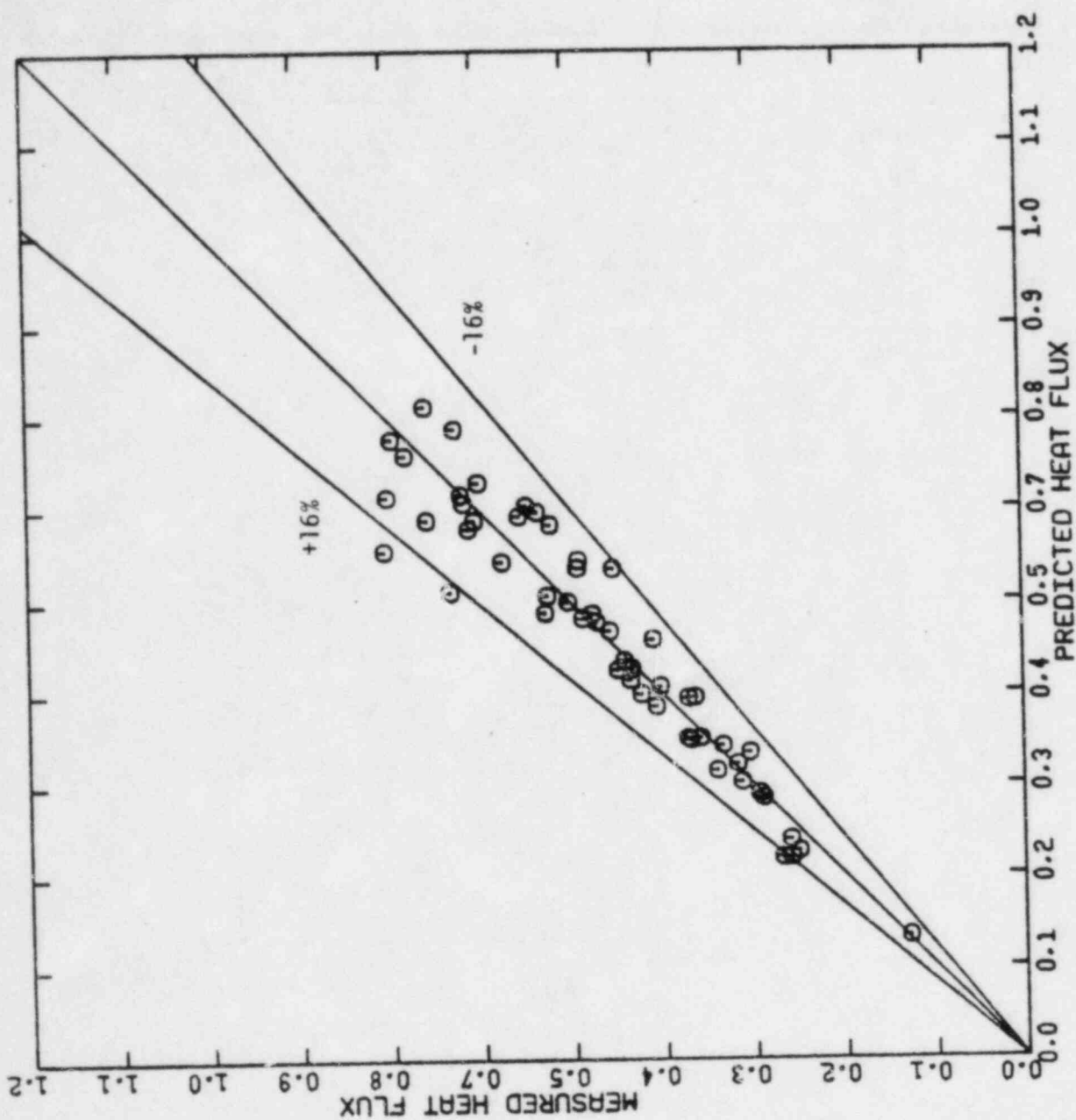
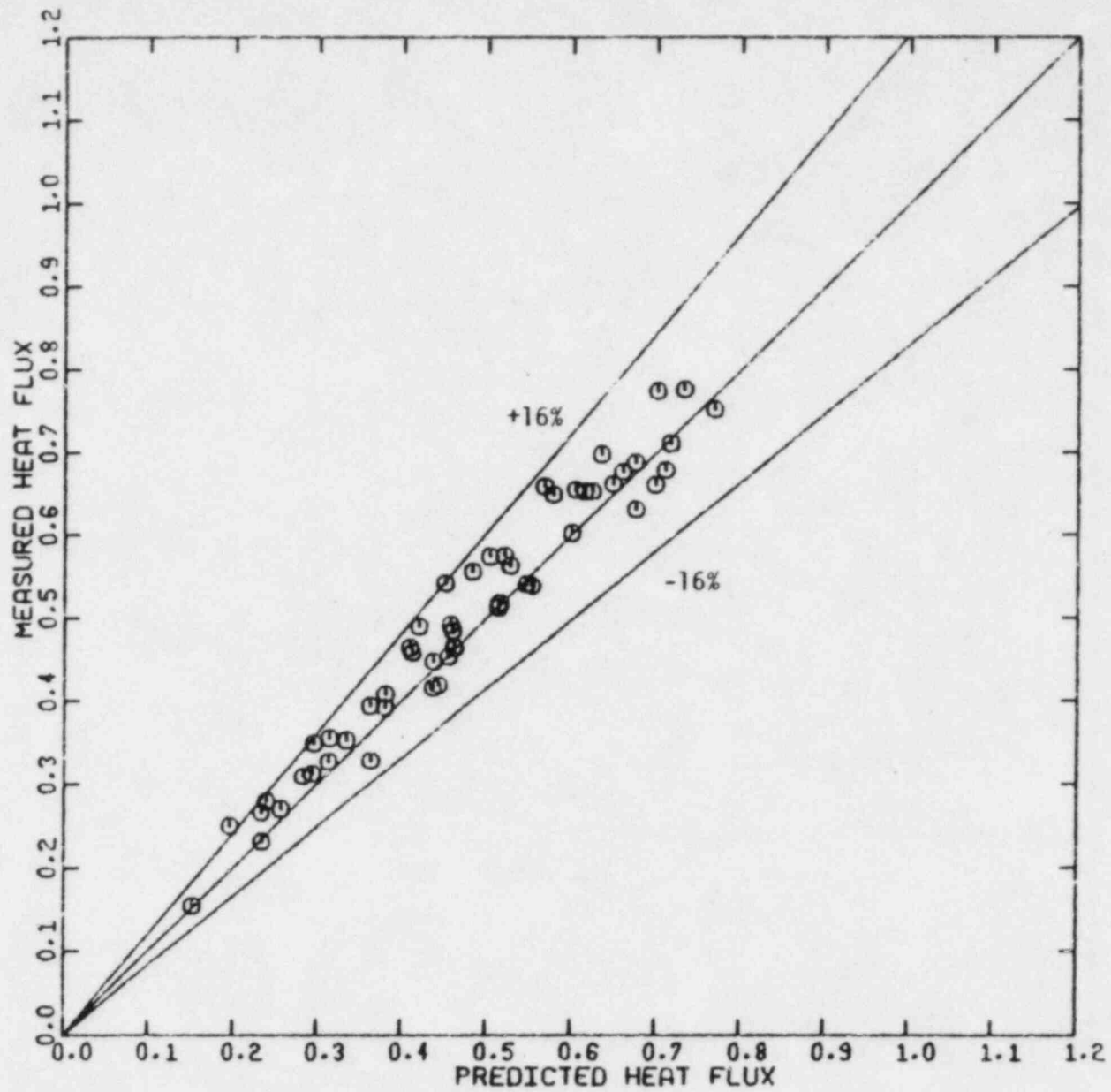


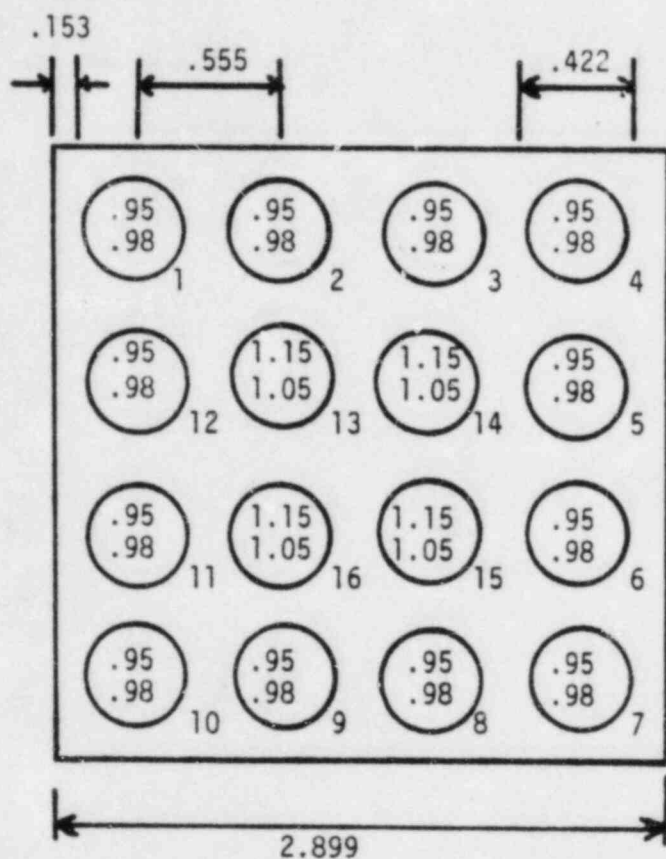
FIGURE 3.27 COMPARISON OF HEAT FLUX - WH-162



3-39

XN-NF-621 (NP)(A)
Revision 1

FIGURE 3.28 COMPARISON OF HEAT FLUX - WH164



UPPER POWER FOR TEST SECTIONS 2,6
LOWER POWER FOR TEST SECTIONS 7,8.

NUMBER OUTSIDE SHOWS ROD NUMBER

Figure 3.29 Test Section Geometry and Local Power Distributions for ROSAL 2, 6, 7 and 8 Test Assemblies

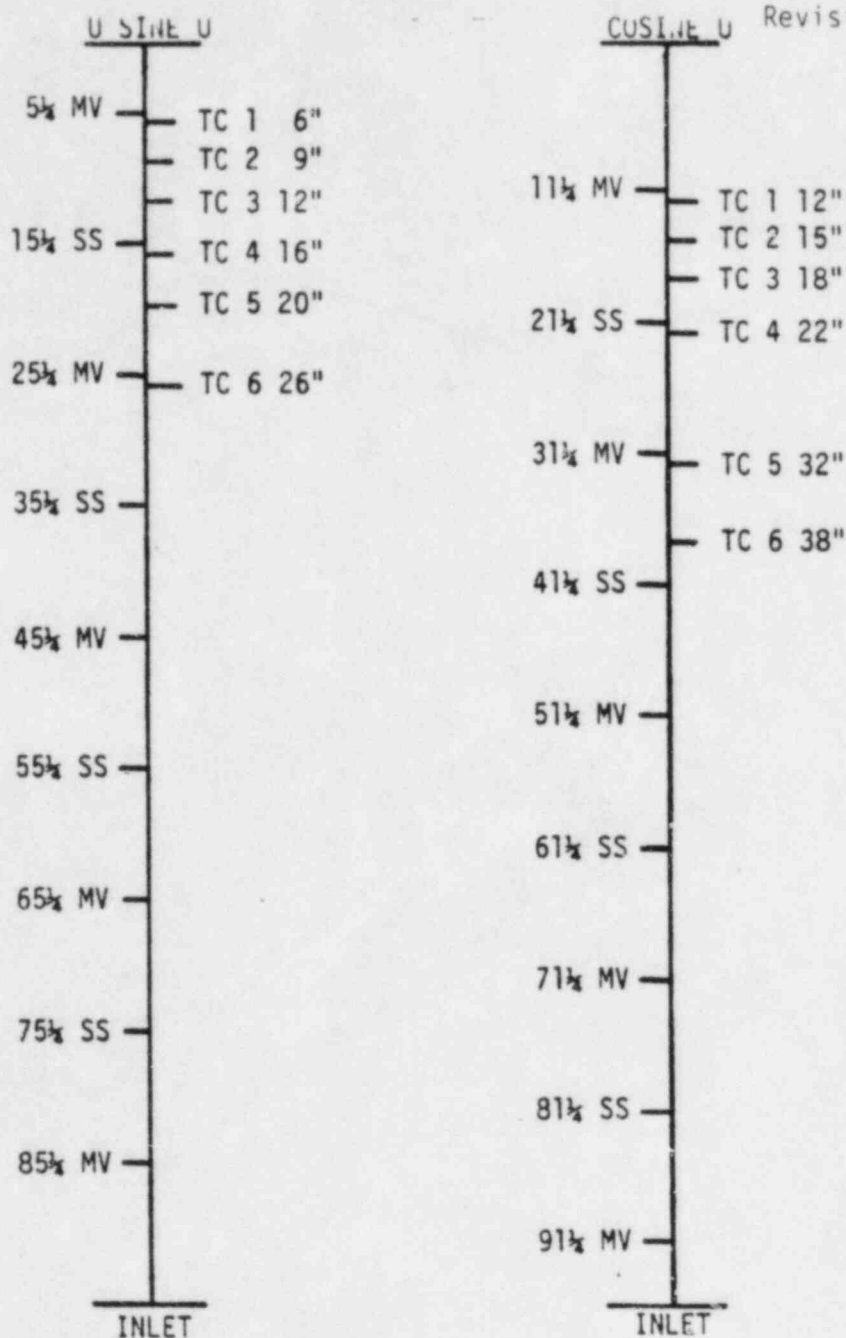


Figure 3.30 Spacer and Thermocouple Locations for ROSAL 2, 6, 7 and 8 Test Sections; MV = Mixing Vane Grid; SS = Simple Support and TC = Thermocouple Location. Distances From End of Heated Length.

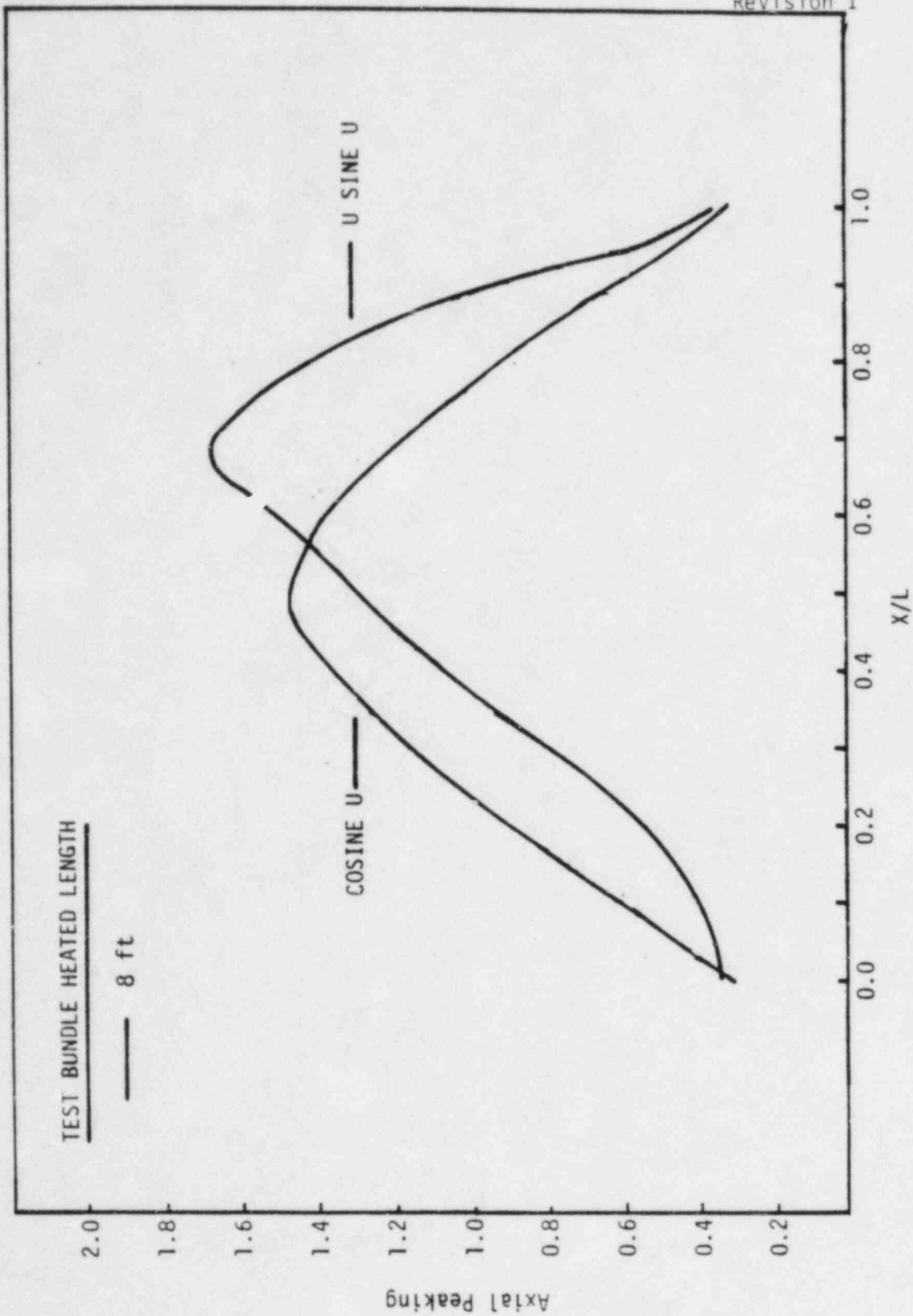


Figure 3.31 Axial Power Distributions For ROSAL Data

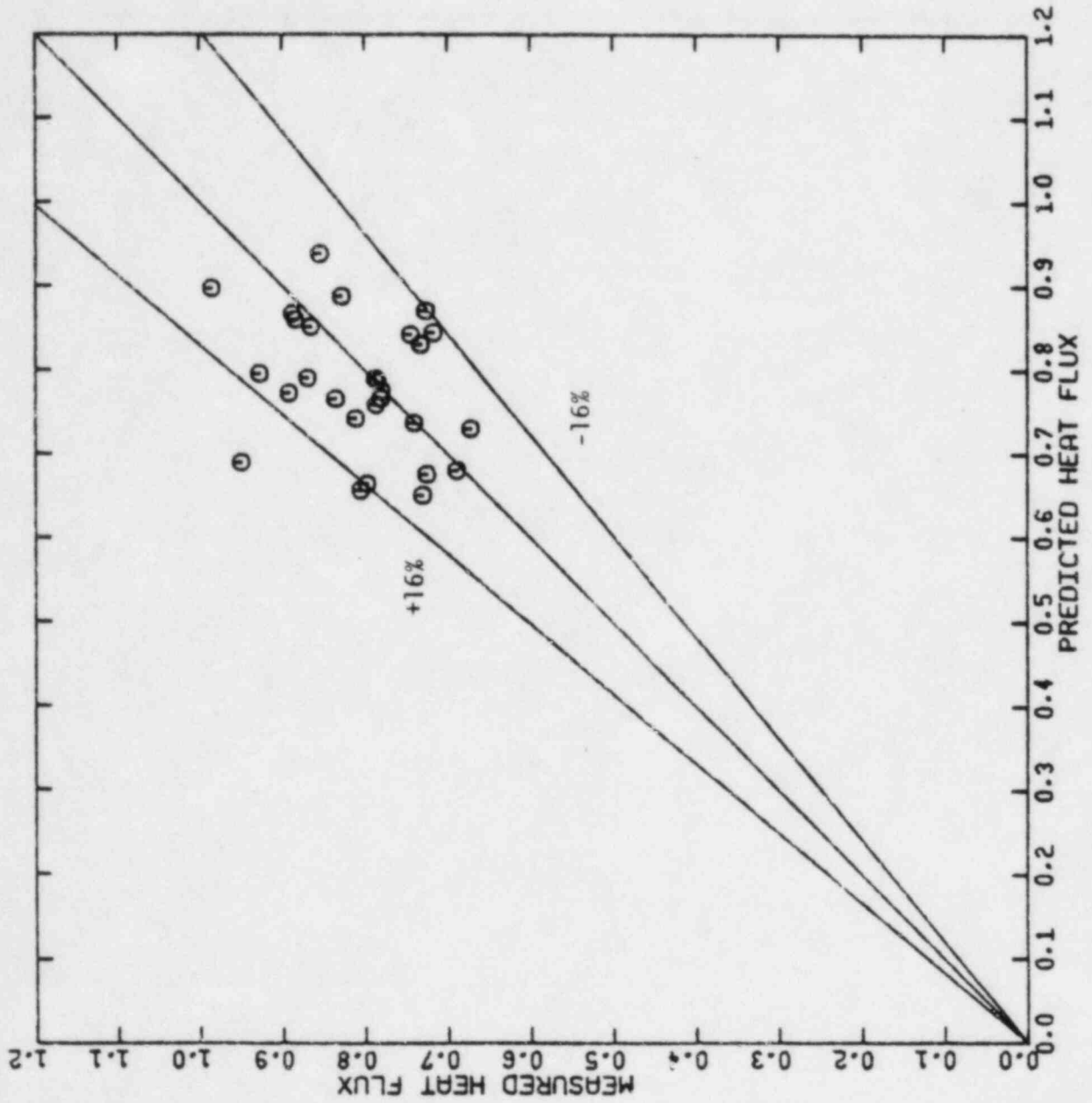


FIGURE 3.32 COMPARISON OF HEAT FLUX - ROSAL . 2

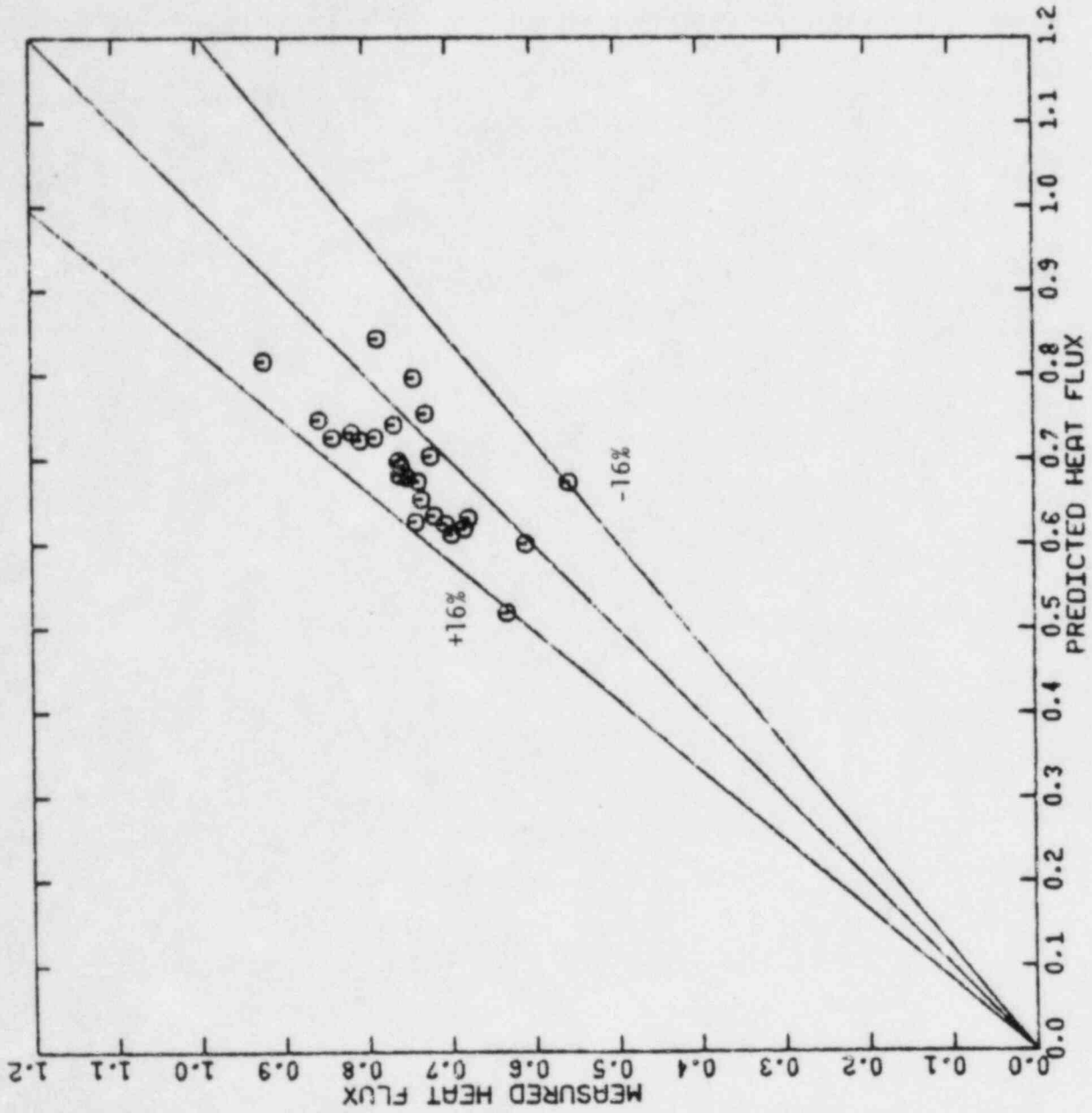
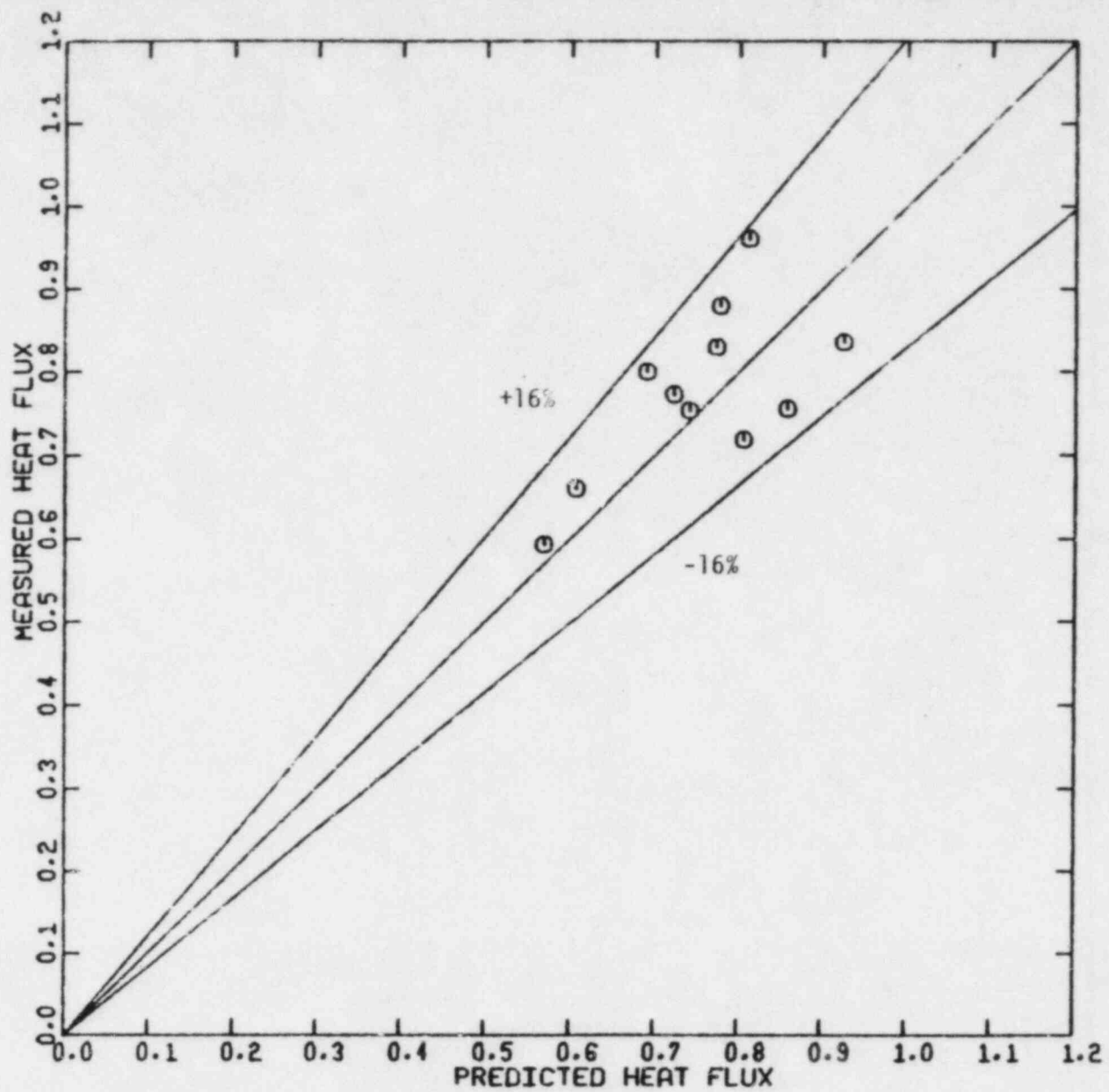


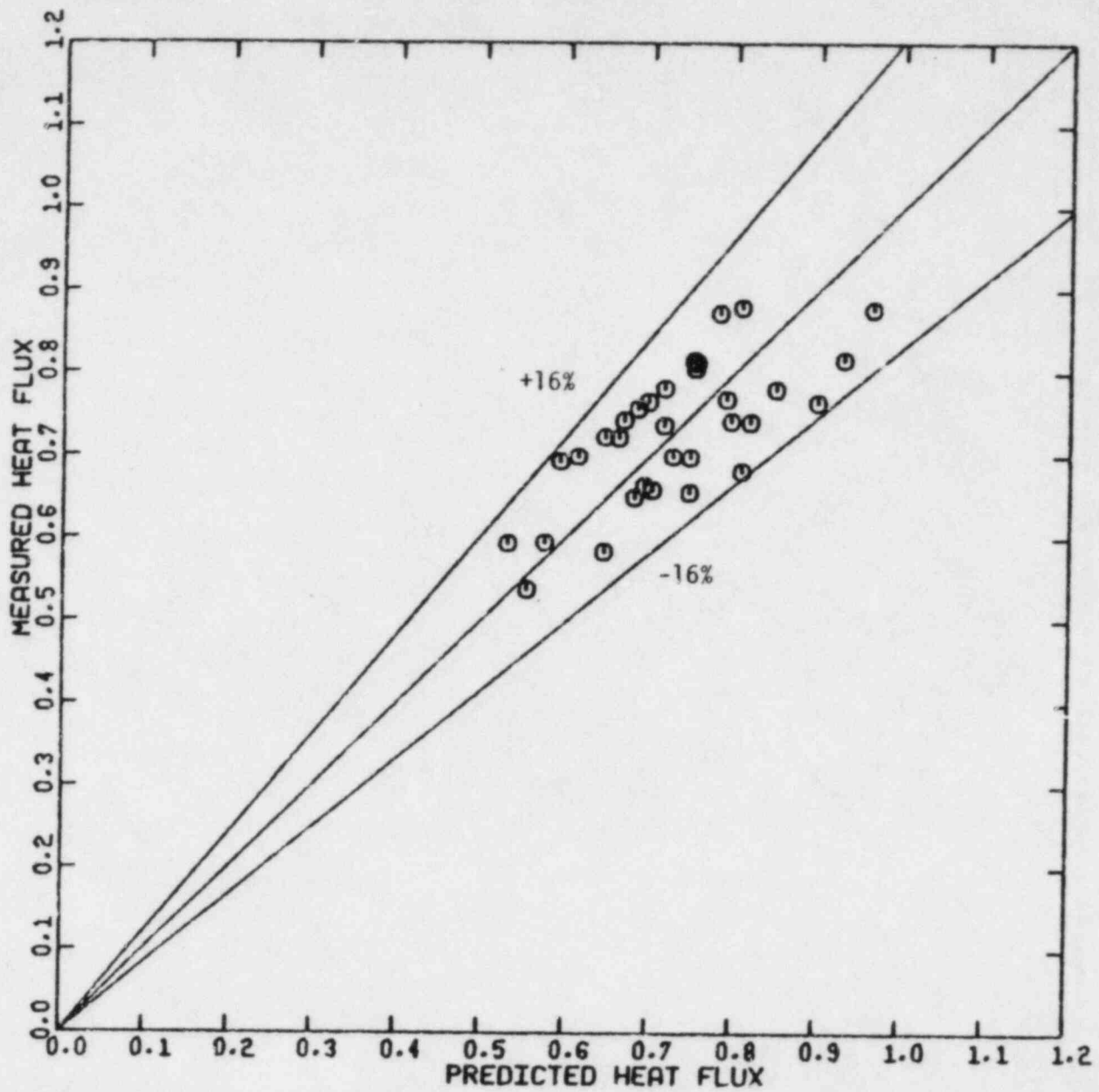
FIGURE 3.33 COMPARISON OF HEAT FLUX - ROSAL.4



3-45

XN-NF-621 (NP)(A)
Revision 1

FIGURE 3.34 COMPARISON OF HEAT FLUX - ROSAL.7



3-46

XN-NF-621 (NP) (A)
Revision 1

FIGURE 3.35 COMPARISON OF HEAT FLUX - ROSAI . 8

4.0 STATISTICAL EVALUATION

The experimental data were used to determine the departure from nucleate boiling ratio criterion, u , which satisfies the following statistical statement: With 95% confidence, at least 95% of the population of DNBR are less than u . This is referred to as a 95/95 tolerance statement.

Calculational steps for computing u are outlined below. From the estimates of means and standard deviations for the individual test sections an estimate of the overall mean (a weighted average)* and the overall standard deviation, σ_T , are determined. Two variance components are calculated:

- (1) The within test section variance, σ_W^2
- (2) The between test section variance, σ_B^2

The tolerance interval is constructed by methods given by Weissberg and Besty.⁽¹⁰⁾ The interval requires knowledge of the degrees of freedom associated with $\sigma_T^2 (= \sigma_W^2 + \sigma_B^2)$, and the effective sample size, N , for the estimate of the weighted average.

The degrees of freedom for σ_T are found by Satterthwaite's formula⁽¹¹⁾ to be 396. The effective sample size, N , is the number of observations required to be selected at random from the population to give an estimate of having a variance of .00010586, which is the variance of the weighted average. The value of N is found by solving:

* The weighted average is based on the number of data points of each test section and the relative sizes of the variance between and within test sections.

$$\frac{\sigma_T^2}{N} = .00010586$$

The limit for u is then derived from

$$u = \mu + K\sigma_T$$

where K is given in Reference 13. Therefore, the tolerance statement becomes:
With 95% confidence at least 95% of the DNBR (predicted to measured DNB heat flux) values are less than 1.16 for all the data analyzed.

5.0 REFERENCES

- (1) K.P. Galbraith and T.W. Patten, "XCOBRA-IIIC: A Computer Code to Determine the Distribution of Coolant During Steady State and Transient Core Operation," XN-75-21.
- (2) R.B. Macduff and T.W. Patten, "DNB Test Data Report," XN-NF-81-80, Revision 1, January 15, 1982.
- (3) C. Fighetti and D. Reddy, "Compilation of Critical Heat Flux Data Taken at Columbia University," to be published as EPRI Report EPRI Project RP-813.
- (4) T.W. Patten, "Test Specification for a 17x17 DNB Test Program," XN-NF-P62,659, July 1980.
- (5) M.G. Hartman, "Analysis of the Palisades DNB and Mixing Tests," XN-75-65(P), January 1976.
- (6) C.E. Leach, "Departure From Nucleate Boiling Test Specification," XN-S30207, Revision 1.
- (7) J. Yates, "H.B. Robinson Departure From Nucleate Boiling Test Analysis and Results," XN-75-45, October 20, 1975.
- (8) K.P. Galbraith, T.W. Patten, J.L. Jaech and M. McMullen, "Definition and Justification of Exxon Nuclear Company DNB Correlation for PWR's," XN-75-48, October 1975.
- (9) R.B. Macduff, "Turbulent Mixing in Rod Bundles," XN-NF-81-73, October 1981.
- (10) A. Weissberg and G.H. Beatty, "Tables of Tolerance Limit Factors for Normal Distributions," Technometrics 2 No. 4 483-500, November 1960.
- (11) F.E. Satterthwaite, "An Approximate Distribution of Estimate of Variance Components," Biometrics Bulletin 2, 1946.
- (12) L.S. Tong, "Boiling Crisis and Critical Heat Flux," AEC Critical Review Series, 1972.
- (13) D. B. Owen, "Factors for One-Sided Tolerance Limits," SCR-607, March 1963.
- (14) E.R. Rosal, J. Cermak, L. Tong, J. Casterline, S. Kokolis, B. Matzner, "High Pressure Rod Bundle DNB Data With Axially Non-Uniform Heat Flux," Nuclear Engineering and Design, 31 (1974) pp. 1-20.

B-1

XN-NF-621 (NP)(A)
Revision 1

DATA SUMMARY FOR TEST SECTION - ROSAI-2

CASE	PRESSURE	MASS FLUX	INLET	LOCAL	HEAT FLUX		MDNBR
	PSIA	MLB/HRFT ²	SUBCOOLING	ENTHALPY	MEASURED	PREDICTED	
			BTU/LBM	BTU/LBM	MBTU/HRFT ²	MBTU/HRFT ²	

0.726
0.866
0.915
1.134
1.072
1.198
0.857
0.815
0.995
0.984
0.987
0.972
0.976
0.965
0.931
0.833
0.917
0.891
0.910
0.982
0.911
1.002
1.099
0.996
1.003
1.131
1.086
1.177

C-6

XN-NF-621 (NP)(A)
Revision 1

DATA SUMMARY FOR TEST SECTION - CE-59

CASE	PRESSURE PSIA	MASS FLUX MLB/HRFT2	INLET SUBCOOLING BTU/LBM	LOCAL ENTHALPY BTU/LBM	HEAT FLUX		MDNBR
					MEASURED MBTU/HRFT2	PREDICTED MBTU/HRFT2	
-----							1.039
						1.169	
						0.961	
						0.925	
						1.063	
						0.957	
						0.998	
						1.028	
						0.958	

C-8

XN-NF-621 (NP)(A)
Revision 1

DATA SUMMARY FOR TEST SECTION - WH-162

CASE	PRESSURE PSIA	MASS FLUX MLB/HRFT ²	INLET SUBCOOLING BTU/LBM	LOCAL ENTHALPY BTU/LBM	HEAT FLUX		MDNBR
					MEASURED MBTU/HRFT ²	PREDICTED MBTU/HRFT ²	

1.182
1.028
1.087
1.120
0.985
1.103
0.789
0.945
1.122
1.091
0.808
1.104
1.115

XN-NF-621(NP)(A)
Revision 1
Issue Date 10/21/83

EXXON NUCLEAR DNB CORRELATION
FOR PWR FUEL DESIGNS

DISTRIBUTION

J. C. Chandler
R. B. Macduff
J. N. Morgan
J. C. Chandler/NRC (16)
Document Control (5)